Catarina Teixeira Toste

Bachelor in Cell and Molecular Biology

Development of a new biophotocatalytic system for biofuel production

Dissertation for the obtention of Master's degree in Biotechnology

Supervisor: Dr. Inês Cardoso Pereira, Full Professor, ITQB NOVA

Co-supervisor: Dr. Mónica Martins, Researcher, ITQB NOVA

Jury

President: Prof. Dr. Carlos Salgueiro, FCT NOVA

Opponent: Dr. Vânia Brissos, ITQB NOVA

Vowel: Dr. Mónica Martins, ITQB NOVA

FACULDADE DE
CIÊNCIAS E TECNOLOGIA
UNIVERSIDADE NOVA DE LISBOA

December 2020

Catarina Teixeira Toste

Bachelor in Cell and Molecular Biology

Development of a new biophotocatalytic system for biofuel production

Dissertation for the obtention of Master's degree in Biotechnology

Supervisor: Dr. Inês Cardoso Pereira, Full Professor, ITQB NOVA

Co-supervisor: Dr. Mónica Martins, Researcher, ITQB NOVA

December 2020

Development of a new biophotocatalytic system for biofuel production

Parts of this work are reported in a research article under review:

"Enhanced light-driven hydrogen production by self-photosensitized biohybrid systems" by Mónica Martins, Catarina Toste, Inês A.C. Pereira

"É preciso sair da ilha para ver a ilha.
Não nos vemos se não saímos de nós."

José Saramago

To my amazing family.

Agradecimentos

Primeiramente, quero agradecer às minhas orientadoras Dr.ª Inês Cardoso Pereira e Dr.ª Mónica Martins por me terem dado uma oportunidade e acreditado em mim, por todos os ensinamentos, conselhos e palavras de apoio transmitidas, um muito obrigado! Quero expressar a minha especial gratidão à Dr.ª Mónica, por me acompanhar e orientar ao longo destes meses, pela confiança depositada, por estar sempre disponível para esclarecer as minhas dúvidas, por não me deixar desanimar e por fim por compartilhar seus conhecimentos, entusiasmo e otimismo, o meu sincero obrigado!

Aos meus colegas de laboratório Rita, Ana, Delfim, Américo, Ritinha, Margarida e Renato, pela simpatia, por não hesitarem em ajudar ou dizer uma palavra amiga sempre que preciso, por me fazerem sentir em casa e me acolherem tão BEM no grupo, obrigada! Aos meus colegas de mestrado Gonçalo e Henrik, por partilharem comigo esta aventura, por me apoiarem e me contagiarem com boa disposição e alegria.

Também quero agradecer aos meus companheiros de almoço Gonçalo, Salomé, Jessica, Rita, Laura e Jheny pelas conversas (sempre muito animadas!) e por todo o encorajamento e força.

Não poderia passar sem expressar o meu profundo obrigado às minhas colegas de casa Ana, e em especial à Géssica, pela amizade, pelas palavras de encorajamento, por me animarem nestes tempos mais difíceis e pelos magníficos cozinhados e conversas!

Às minhas queridas amigas Marta, Andreia, Jessica e Ana por estarem sempre lá nos bons e maus momentos, por serem pessoas incríveis pela qual sou

muito grata. Aos meus amigos, na impossibilidade de agradecer a todos individualmente, um grande obrigado pelo apoio e compreensão.

Por fim quero deixar um agradecimento muito especial a toda a minha família. Por serem o meu maior pilar, fonte de conforto e por fazerem de mim o que sou hoje! Pelo carinho, força e amor incondicional que foram indispensáveis ao longo deste meu percurso, por nunca o deixaram esquecer mesmo estando longe, por tudo isso um enorme OBRIGADO!

Abstract

Currently, global energy requirements rely heavily on fossil fuels, the primary contributors to global warming and severe climate changes. It is imperative to decarbonize the energy supply sector, by utilizing an alternative, clean and sustainable energy source, like hydrogen, that can be generated from renewable resources, such as solar energy. The aim of this dissertation was the construction of a new biophotocatalytic system using non-photosynthetic anaerobic bacteria coupled with semiconductor metal sulfide nanoparticles, for light-driven H_2 production. In this system, nanoparticles act as light-harvesting material, enabling the microorganism to capture and absorb sunlight energy, using it for H_2 generation. In the present work, four bacteria *Citrobacter freundii*, *Clostridium acetobutylicum*, *Desulfovibrio vulgaris* and *Desulfovibrio desulfuricans* were used as biocatalysts with self-produced cadmium sulfide (CdS) nanoparticles to produce hydrogen. The performance of these biohybrids was further compared with the control system *Escherichia coli*-CdS. Moreover, new semiconductor combinations were tested, by loading cocatalysts metals tungsten (W), nickel (Ni) and molybdenum (Mo) into CdS. The *D. desulfuricans*-CdS biohybrid was demonstrated to be the best photocatalytic system for light-driven H_2 production from the four biohybrids proposed and *E. coli*-CdS control system. *D. desulfuricans*-CdS system presented a remarkable H_2 production both in the presence and absence of the electron mediator methyl viologen (MV), with 46.0±4.8 and 31.7±8.1 µmol of H_2, respectively, after 45 and 142 h of light irradiation. The *D. desulfuricans*-CdS performance was improved by adding cocatalysts, especially Mo, that allowed the increase of H_2 production rate from 34.0±0.8 to 130.8±9.3 µmol $g_{dcw}^{-1}h^{-1}$, without MV. Finally, *D. desulfuricans*-CdS-MoS_2 was successfully immobilized in calcium alginate beads and a batch photoreactor for H_2 production was constructed. These results show the high potential of *D. desulfuricans*-CdS-MoS_2 biohybrid photosystem for an efficient and clean hydrogen production.

Keywords: Hydrogen production, photocatalysis, non-photosynthetic bacteria, self-photosensitization, biogenic nanoparticles, cocatalysts

Resumo

Atualmente, as necessidades energéticas globais dependem fortemente da utilização de combustíveis fósseis, os principais responsáveis pelo aquecimento global e alterações climáticas severas. É imperativo descarbonizar o setor de abastecimento de energia, utilizando uma fonte de energia alternativa, limpa e sustentável, como o hidrogénio, que pode ser gerado a partir de um recurso renovável: energia solar. O objetivo desta dissertação consistiu na construção de um novo sistema bio-fotocatalítico utilizando bactérias anaeróbias não-fotossintéticas acopladas a nanopartículas semicondutoras de sulfureto metálico, para produção de H_2, usando luz como fonte de energia. Neste sistema, as nanopartículas atuam como semicondutor para captar a energia solar, transferindo-a para o microrganismo que a utiliza para gerar H_2. No presente trabalho, as quatro bactérias *Citrobacter freundii*, *Clostridium acetobutylicum*, *Desulfovibrio vulgaris* e *Desulfovibrio desulfuricans* foram utilizadas como biocatalisadores em conjunto com nanopartículas de sulfureto de cádmio (CdS), produzidas pelas mesmas, para a produção de hidrogénio. O desempenho destes biohíbridos foi posteriormente comparado com o sistema de controlo, *Escherichia coli*-CdS. Para além disso, novas combinações de semicondutores foram testadas, acoplando os metais co-catalisadores: tungsténio (W), níquel (Ni) e molibdénio (Mo) ao CdS. O biohíbrido *D. desulfuricans*-CdS demonstrou ser o melhor sistema fotocatalítico para a produção de H_2 através da luz, dos quatro biohíbridos propostos e do sistema controlo *E. coli*-CdS. O sistema *D. desulfuricans*-CdS apresentou uma produção significativa de H_2 tanto na presença como na ausência do mediador de eletrões metil viologénio (MV), com 46,0±4,8 e 31,7±8,1 µmol de H_2, respetivamente, após 44 e 142 h de irradiação de luz. O desempenho de *D. desulfuricans*-CdS foi melhorado com a adição de co-catalisadores, principalmente com Mo, que permitiu o aumento da taxa de produção de H_2 de 34,0±0,8 para 130,8±9,3 µmol $g_{dcw}^1 h^1$, sem MV. Finalmente, o sistema *D. desulfuricans* CdS-MoS_2 foi imobilizado, com sucesso, em esferas de alginato de cálcio e foi construído um foto-reator em *batch* para produção de H_2. Estes resultados demonstraram o elevado potencial do fotossistema biohíbrido *D. desulfuricans*-CdS-MoS_2 para produção eficiente e limpa de hidrogénio.

Palavras-chave: produção de hidrogénio, fotocatálise, bactérias não-fotossintéticas, auto-fotossensibilização, nanopartículas biogénicas, co-catalisadores

Table of Contents

List of Figures

List of Tables

List of Abbreviations

GC   gas chromatography

Hase   hydrogenase

MV   methyl viologen

MFC   microbial fuel cell

NPs   nanoparticles

SRB   sulfate reducing bacteria

SED   sacrificial electron donor

SEM-EDS   scanning electron microscopy and energy dispersive spectroscopy

TMDs   transition metal dichalcogenides

Chemical formulas:

Cd   cadmium
CdS   cadmium sulfide
Fe   iron
H_2S hydrogen sulfide
In   indium
Mo   molybdenum
Ni   nickel
N_2 nitrogen
Pd   palladium
Pt   platinum
S   sulfur

List of Abbreviations

S^{2-}	sulfide
SO_4^{2-}	sulfate
Se	selenium
TiO_2	titanium oxide
W	tungsten

Chapter 1: Introduction

The increase of global energy demand, due to growth of world's population coupled with the rise of living standards, has become one of the major challenges of 21st century[1,2]. Currently, 85.5% of worldwide energy requirements are fulfilled by fossil fuels, a non-sustainable energy source with a massive environmental impact[3]. The utilization of fossil fuels involves its combustion that, in turn, results in greenhouse gases emissions (mainly CO_2), the major cause of global warming and extreme climate changes. Therefore, it is essential to decarbonize energy supply by using an alternative, sustainable and renewable energy source.[1–4]

Hydrogen is a clean and versatile energy carrier, that can be easily stored and transported over long distances and periods of time[1,5,6]. It presents a broad spectrum of applications: from fuel source for transportation and energy storage (for power and heat generation), to an important chemical feedstock in several industrial processes (such as methanol and ammoniacal production to petroleum and metals refinery) (**Figure 1.1**.).[4–8] Hydrogen is often recognized as the ideal fuel since it is a clean energy source (its combustion yields only water) and because of its high energy content (~142 kJ g^{-1}), which is three times greater than hydrocarbon fuels energy[8–11].
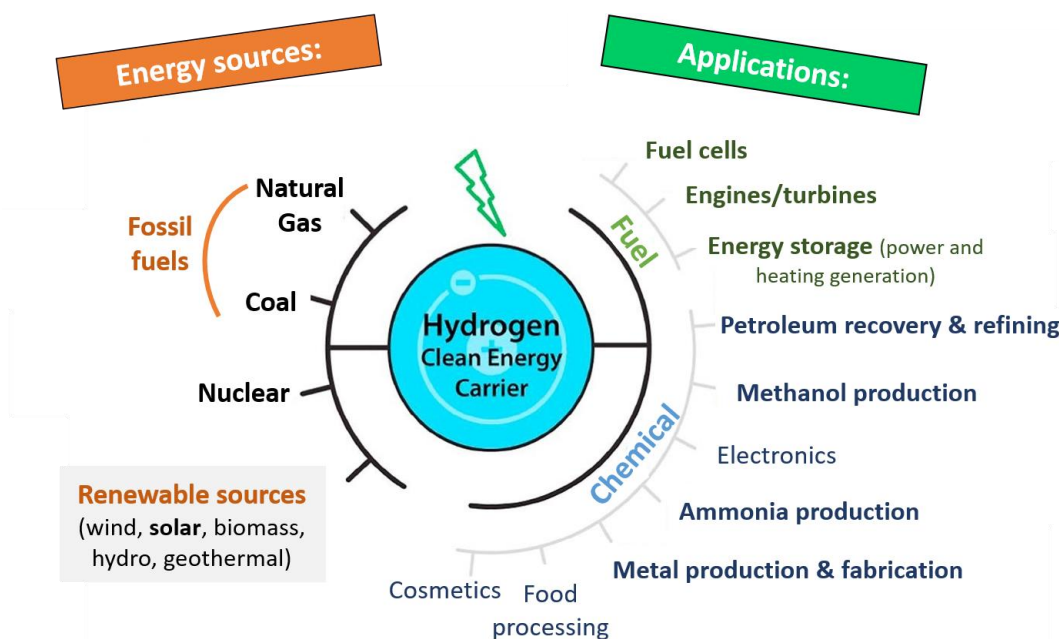
Figure 1.1.- Hydrogen - energy sources and applications. Adapted from[8].

Although, H_2 production is still primarily based on fossil fuels resources (particularly from natural gas and coal), it can also be generated from renewable sources (**Figure 1.1.**).[8,11,12] Solar energy is an inexhaustible, non-polluting and the most abundant energy resource, thereby making solar hydrogen production an attractive option towards a low-carbon and sustainably energy economy[13–15]. Thus, biological hydrogen production from solar energy is one approach that has been investigated.

1.1. – Biological solar hydrogen production

Solar-driven H_2 production is naturally performed by specific photosynthetic organisms (e.g. algae and cyanobacteria), under anaerobic conditions[16]. Hydrogen photoproduction is attained by diverting the photogenerated electrons obtained via photosynthesis towards hydrogenases (Hases)[16–19], that catalyze the reversible conversion of two protons and electrons into H_2 (**Equation 1.1.**)[20]:

$$2\,H^+ + 2\,e^- \leftrightarrow H_2 \qquad (\textbf{Equation 1.1.})$$

Since photosynthetic organisms prioritize survival strategies rather than converting sunlight for chemicals production, the efficiency of solar hydrogen production is very low for those species[21]. Additionally, the photosynthetic process achieves its saturation at solar intensities considerably below the full flux (~20 % of solar intensity), a cellular mechanism that helps preventing photodamage of the photosynthetic system[21,22]. Furthermore, the inhibition of Hases in presence of O_2 as well as the need of diffusional electron donors (e.g. ferredoxins) to allow electron transfer for PSI (photosystem I) to Hases, are major drawbacks in scalability of solar-driven H_2 production via biological route[16–18]. Therefore, an alternative method for H_2 production is required to overcome these limitations, like semi-artificial photosynthesis systems.

1.2. – Semi-artificial photosynthesis systems

Semi-artificial photosynthesis is an innovative hybrid strategy that aims to combine the excellent light-harvesting efficiency of synthetic materials, with the high specificity of biocatalytic machinery (enzymes or microorganisms), for solar-to-chemicals conversion[17,21,23]. In this photosynthetic biohybrids, the inorganic semiconductor is used to absorb and capture solar energy, whereas the biological component catalyzes its subsequent conversion to chemical energy.[21–24] Hence, several semi-artificial photosynthesis systems have been developed for H_2 production (**Figure 1.2.**).
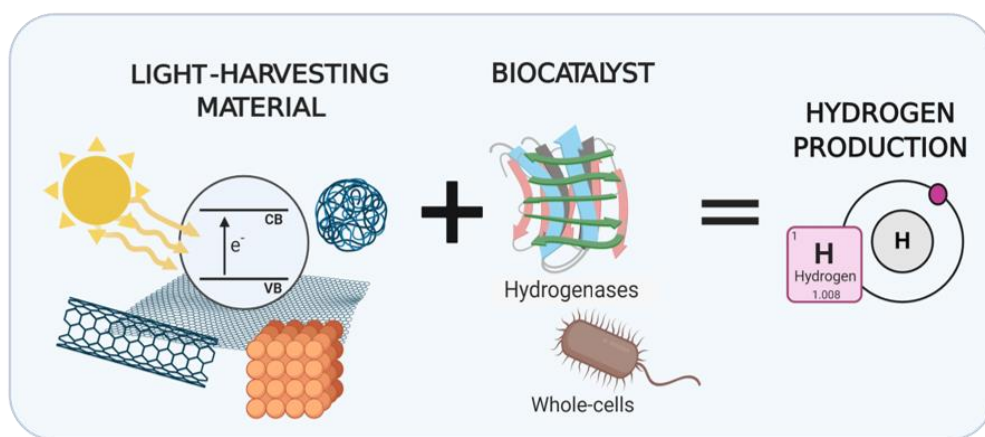
Figure 1.2.- Schematic representation of semi-artificial photosynthesis for H_2 production. Created with Biorender.com.

The majority of the biohybrids created for hydrogen photoproduction employed light-harvesting materials with hydrogenases as biocatalysts (**Figure 1.2**)[25]. One example of hydrogenase studied in semi-artificial photosynthesis is [NiFeSe]-Hase from *Desulfovibrio vulgaris* Hildenborough bacterium[26–28]. [NiFeSe]-Hase has been integrated in a lead halide perovskite solar cell[26], as well as coupled with synthetized PSI monolayer photocathode[27], for solar water splitting purposes. Moreover, this enzyme had also been combined with indium (III) trisulfide (In_2S_3) semiconductor particles for visible light-driven H_2 production[28].

However, the inherent enzyme instability and the costly and time-consuming manipulations involved (e.g. isolation and protein purification), have restrict their commercial application[17,21,24]. Thus, to overcome these limitations, photosynthetic biohybrids systems have recently started to be developed using whole-cells as biocatalysts (**Figure 1.2.**). Microorganisms are not only a more versatile catalyst – synthetizing more complex products (due to their diverse biosynthetic pathways) with high specificity and efficiency, – but are also more stable than isolated enzymes. Additionally, the self-repair and reproductive nature of microorganisms enables cell hybrids prospects for scalability.[17,22,24]

Initial studies of whole-cell biohybrids explored the potential of different bacteria such as *Clostridium butyricum*, *Rhodopseudomonas capsulata* and *Rhodospirillum rubrum* as biocatalysts for photocatalytic H_2 production. These organisms were then coupled with a semiconductor, namely titanium oxide (TiO_2) or bismuth oxide (Bi_2O_3), in presence of a redox mediator (that transfer electrons from semiconductors to bacteria)[29–31]. Recently, microbial hybrid systems employing genetically engineered *Escherichia coli* with anatase TiO_2 as semiconductor or *E. coli* conjugated with TiO_2 nanoparticles, have also been developed for light-driven H_2 production, using an electron shuttle as well[32–34]. Moreover, a similar approach was investigated using electroactive *Shewanella oneidensis* bacterium and water-soluble photosensitizers to produce H_2 and reduce fumarate, pyruvate, and CO_2 to formate[19]. However, in this methodology a direct interaction between cells and light-harvesting materials does not occur,

thus requiring an electron-mediator.[17] Moreover, these biohybrid systems integrate chemically-produced semiconductors, whose synthesis often requires complex and energy-intensive techniques[35–38]. Alternatively, a recent and interesting strategy of semi-artificial photosynthesis has been developed: Self-photosensitization of non-photosynthetic bacteria.

1.3. – Self-photosensitization of non-photosynthetic bacteria

In this new approach the biohybrids systems are constructed by photosensitizing non-photosynthetic microbes with self-produced metal semiconductor nanoparticles, for solar-to-chemical production, using visible light as energy source (**Figure 1.3.**).[21,39]
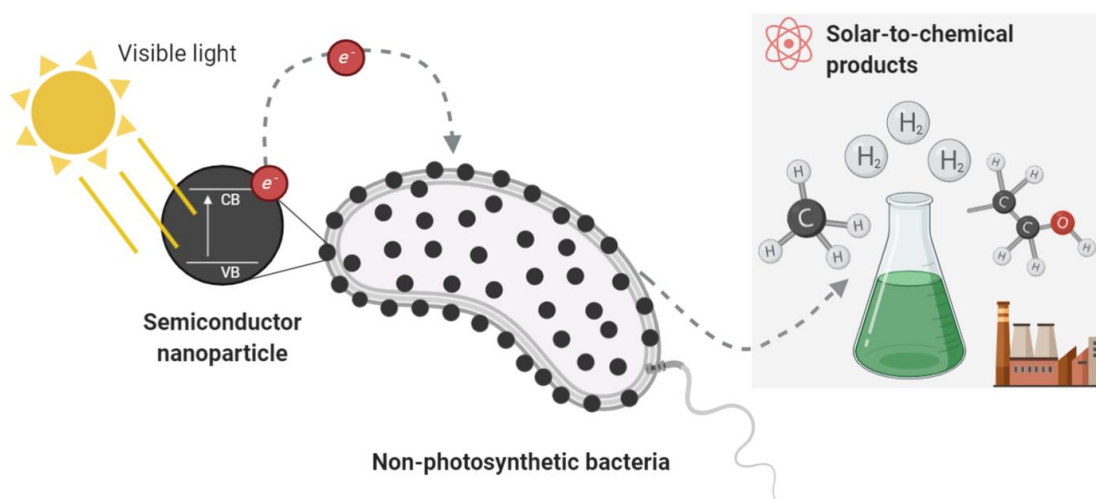
Figure 1.3.- Schematic representation of self-photosensitization of non-photosynthetic bacteria strategy for solar-to-chemical production. Created with Biorender.com.

Non-photosynthetic organisms can harbor pathways for more diverse and complex products, than photosynthetic ones, due to its efficient and alternative CO_2 fixation and reduction pathways[40–42]. Moreover, nanostructured materials recently emerged as attractive light-harvesting semiconductors for photosynthetic biohybrid systems[22,43]. Nanoparticles (NPs) present a high potential as light harvester due to their: *1)* visible-light absorption capacity and

tuneability of charge separation, *2)* increased surface-to-volume ratio (providing a larger area for photocatalytic reactions to occur), *3)* ease of interaction with biological systems (due to their similar dimensions) and *4)* biocompatibility with biocatalysts[22,24,43,44]. Thus, incorporating nanomaterials into living organisms has the potential to enhance or even enable completely new functions of biological systems[21,45].

Hence, this innovative strategy has been designed for solar-to-chemical applications, particularly for CO_2 reduction and H_2 production:

1.3.1.- Biohybrid systems for light-driven CO_2 reduction

In 2016, Sakimoto and coworkers pioneered this approach in a landmark study where they use non-photosynthetic bacteria *Moorella thermoacetica* and its biologically produced cadmium sulfide (CdS) nanoparticles, to enable photosynthesis of acetic acid from CO_2. In this system, CdS NPs self-precipitated on the cell surface of *M. thermoacetica*, allowing nanoparticles to act as an efficient light-harvesting semiconductor. CdS nanoparticles not only captured solar energy, but also delivered electrons directly to acetogen bacterium, enabling CO_2-to-acetate conversion (via Wood-Ljungdahl pathway) by biocatalyst. This strategy took advantage of natural detoxification mechanisms of *M. thermoacetica* for toxic metals, to induce CdS precipitation, that required the addition of a sulfur source, namely cysteine, to generate the NPs.[39] Thus, this biohybrid represented a cost-effective, self-repair and replicating system for selective CO_2 photoreduction, without the need of a redox mediator and also an environmentally friendly method for semiconductor generation[39,46].

Inspired by this concept, other CdS-biohybrids systems have been developed for light-driven CO_2 reduction, to produce a high diversity of valuable chemicals[17,23,43]. The model methanogen and anaerobic microbe *Methanosarcina barkeri* coupled with its self-produce CdS nanoparticles was employed as the catalytic machinery for direct CO_2 conversion to methane[47]. Another example is the photosynthetic bacterium *Rhodopseudomonas palustris* (*R. paulustris*) and its CdS bio-generated nanoparticles used for CO_2 fixation. Under visible light, *R.*

palustris-CdS biohybrid generated additional reducing equivalents (NADPH), that not only promoted the increase of biomass and photosynthetic efficiency, but also the production of valuable multi-carbon compounds, namely carotenoids and biodegradable thermoplastic poly-b-hydroxybutyrate (PHB)[48]. Additionally, Kumar and coworkers developed a tandem biohybrid system by integrating a consortium of four different electroactive bacteria (*Clostridium ljungdahlii*, *Acetobacterium woodii*, *Moorella thermoacetica* and *Pseudomonas aeruginosa*) with CdS biologically synthetize for CO_2 photoreduction. The main product formed by this system was acetic acid, but methanol, ethanol, propionic, butanoic and hexanoic acids were also generated[49].

1.3.2.- Biohybrid systems for light-driven H_2 production

The biohybrid systems were barely explored for H_2 production, where *Escherichia coli* was the only microorganism used as biocatalyst to create these systems (**Figure 1.4.**). Wang *et al.* reported the enhancement of hydrogen production of non-photosynthetic *E. coli* by inducing self-precipitation of CdS nanoparticles on its surface (**Figure 1.4. A**)[50]. In their follow-up work, they integrated a heterojunction light harvester composed by $AgInS_2/In_2S_3$ nanoparticles on the surface of *E. coli* for light-driven H_2 production also (**Figure 1.4. B**). In_2S_3 NPs were biologically produced by *E. coli* (triggered by the addition of In^{3+} and cysteine), whereas $AgInS_2$ were anchored on In_2S_3 via in-situ ion exchanged (under mild conditions)[51].

Furthermore, Wei and coworkers genetically engineered *E. coli* cells through in situ biosynthesis of CdS NPs, by using a surface-display heavy metal-binding protein, for H_2 generation (**Figure 1.4. C**). PbrR is a membrane-bound protein with cysteine residues, that selectively absorbs both lead and cadmium ions, thereby allowing the generation of CdS nanoparticles on the outer membrane of *E. coli* cells. Additionally, to extend its aerobic use, the *E. coli*-CdS hybrid system was also encapsulated with biomimetic silica, to protect the O_2-sensitive recombinant hydrogenase (**Figure 1.4. D**)[52].
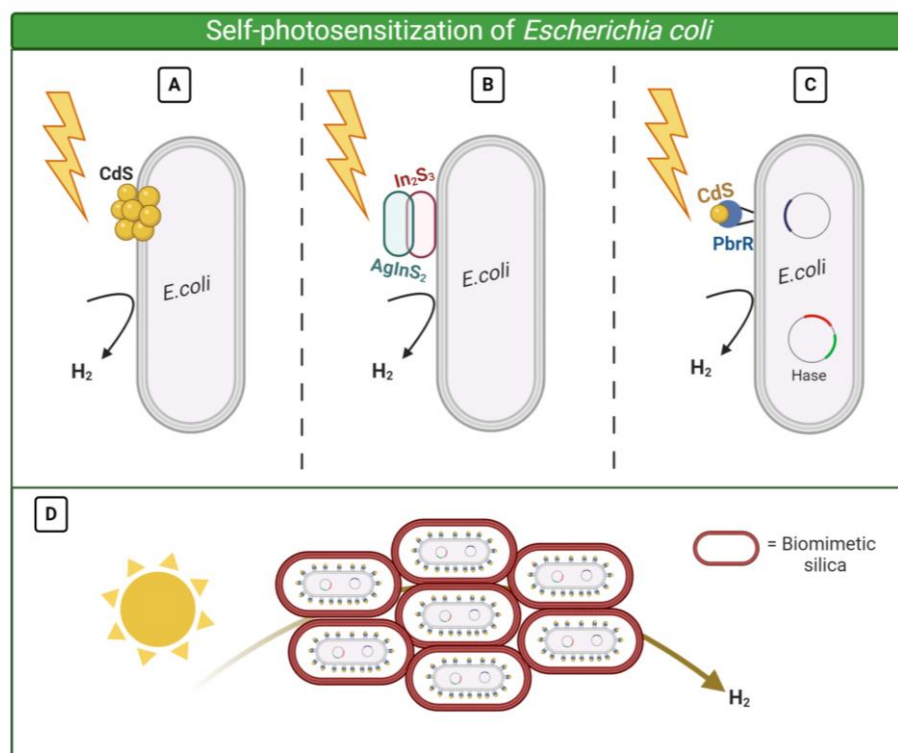
Figure 1.4.- Self-photosensitization of *Escherichia coli* for H_2 photoproduction (state-of-art) with CdS[50] (**A**) and $AgInS_2/In_2S_2$ nanoparticles[51] (**B**). Engineered *E. coli*-CdS system with a surface-display system (**C**) and encapsulated in biomimetic silica[52] (**D**). Created with Biorender.com.

Therefore, these works demonstrated the potential of photosensitizing microorganisms for H_2 production, thus opening a new window of research prospects to further explore this approach. For example, a wider range of microbes could be used as biocatalysts in biohybrid system, particularly those relevant to fuel/chemical production[17]. Furthermore, other light-harvesting materials (or combination of them), to drive electrons to cells, can also be studied to enhance H_2 production by self-photosensitized microorganisms[17,44]. However, these strategies have never been investigated in the scope of photosensitizing microorganisms for light-driven H_2 production, thus we proposed potential non-photosynthetic microorganisms and new semiconductor combinations to create biohybrids systems:

1.3.3.- Potential non-photosynthetic microorganisms to create biohybrids systems

Sulfate reducing bacteria (SRB) is a major and diverse group of anaerobic microorganisms, that are characterized by a high level of hydrogenases and have been reported to produce H_2 from formate (in absence of sulfate)[53–56]. Additionally, since these organisms generate sulfide as a major metabolic product from sulfate respiration, they are thus very efficient in self-production of metal sulfide nanoparticles[57]. *Desulfovibrio vulgaris* and *Desulfovibrio desulfuricans* belong to SRB and present a high potential as biocatalysts for biohybrid system:

Desulfovibrio vulgaris Hildenborough is a well-studied Gram-negative bacterium with its genome sequenced, that has been used as model organism to study the energy metabolism and metal ion bioremediation of SRB[58]. *D. vulgaris* presents seven hydrogenases and has been reported to produce H_2 with high productivity[54–56,59]. The membrane-associated [NiFeSe] hydrogenase of *D. vulgaris* is a strong candidate for biological H_2 production due to its high catalytic rates and resistance to oxygen inactivation[55,60,61]. Additionally, recent studies demonstrated that *D. vulgaris* has the ability to produce biogenic metallic nanoparticles: particularly platinum (Pt) and palladium (Pd) NPs (that were used as catalysts for removal of pharmaceutical compounds) and iron sulfide nanoparticles (FeS NPs), (that enable the extracellular electron uptake by the bacterium from electrodes)[62,63].

Desulfovibrio desulfuricans is a Gram-negative bacterium that presents five hydrogenases and has the ability to produce H_2 through fermentative metabolism[54,56]. In an interesting study of 2011*, D. desulfuricans* was chosen as model organism to study electron transfer processes in microbes and the role of palladium nanoparticles. Thus, *D. desulfuricans* was not only able to biologically synthetize the Pd NPs (bound to the cell membrane), but also to directly transfer electrons to a glassy-carbon electrode (through the self-produced nanoparticles). It was also hypothesized that cytochromes and hydrogenases were involved in

electron transfer to the electrodes[64]. Moreover, other articles used *D. desulfuricans* electroactive biofilms to enhanced current production in Microbial Fuel Cells (MFC), where it was also reported the ability of *D. desulfuricans* to transfer directly electrons to an electrode (anode) by nano-pili structures[65] or via cytochrome c[66].

Additionally, fermentative microorganisms such as *Citrobacter freundii* and *Clostridium acetobutylicum* have a great potential for H_2 production and thus are promising biocatalysts for biohybrid system:

Citrobacter freundii is a Gram-negative bacterium and facultative anaerobic microorganism that belongs to *Enterobacteriaceae* family[67,68]. *C. freundii* is able to produce H_2 under dark fermentation from a wide range of organic compounds (from sugars like glucose and sucrose to lactate)[67–70]. *Citrobacter* species have also been found and isolated from anode biofilms of MFC and reported as electrogenic (that is microorganisms capable of carrying out extracellular electron transfer)[71–73].

Clostridium genus is a large and diverse group of Gram-positive, spore forming and strictly anaerobic bacteria[74,75]. *Clostridium* species, just like *Citrobacter freundii*, can produce H_2 through dark fermentation from a broad spectrum of substrates: from simple carbohydrates (like glucose and sucrose) to degradation of more complex carbohydrates (i.e., cellulose, biomass) derived from industrial wastes or agricultural residues[74–76]. *Clostridium acetobutylicum* contains two monomeric [FeFe] and one [NiFe] hydrogenases[77]. Recently, the existence of cell appendages on *C. acetobutylicum* that can connect the bacterium to an electrode, has been reported for the first time, which can be an important factor in electron transfer processes[78].

Therefore, all these microorganisms have the potential to be used as biocatalysts to create new biohybrid systems.

1.3.4.- Potential semiconductors combinations to create biohybrid systems

Another approach to enhance H_2 production by biohybrid consists in the improvement of the abiotic part of the system, the light-harvesting semiconductor. Several strategies have been employed to enhance its photocatalytic performance for H_2 production, notably by loading cocatalysts on the semiconductor[79–81](**Figure 1.5.**). Cocatalysts can enhance the activity and stability of the semiconductor by *1)* enhancing light-harvesting capacity, *2)* providing active host sites for photocatalytic processes (e.g. H_2 evolution reaction in *water splitting*), *3)* by promoting the separation of photoexcited electrons and *holes* and *4)* by suppressing the inherent photo-corrosion (**Figure 1.5.**)[79–83].
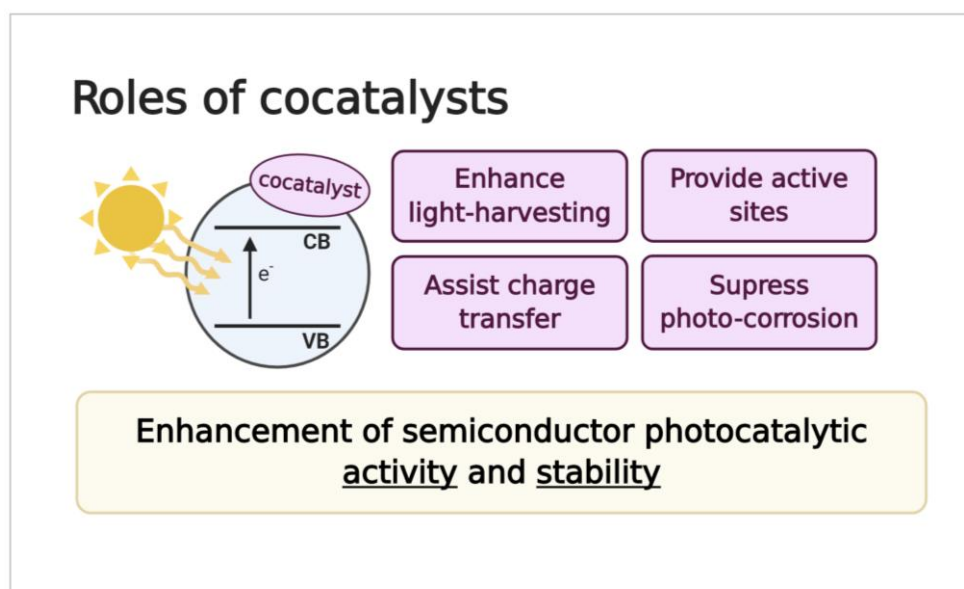
Figure 1.5.- Roles of cocatalysts in photocatalytic H_2 production. Created with Biorender.com

Noble metals (e.g.: Au, Ag, Pd, Pt) are widely used as cocatalysts to increase H_2 production, specially Pt, but its high-costs and limited-reserves are a major drawback for large-scale applications[80,84]. Recently, earth-abundant transition metal dichalcogenides (TMDs) elements, including molybdenum (Mo), tungsten (W) and nickel (Ni), have been considered as an attractive substitute for

nobel-metal-based catalysis, since TMDs also present an efficient catalytic activity and are less expensive and more eco-friendly than nobel metals[79,80,82–86]

Sulfide semiconductors have been widely used for H_2 photocatalysis due to their highly efficient light absorption and fast charge carrier mobility, both characteristic of sulfide[79]. Thus, TMD sulfides have been employed in combination with CdS semiconductor, to improve H_2 production under visible light, resulting in different and interesting binary CdS-based photocatalytic materials[79]. These new structures are constructed via chemical-synthesis. Molybdenum disulfide (MoS_2) is the most studied and frequently used TMD cocatalyst for H_2 photocatalytic production[83,87]. In 2008, Zong *et. al* reported for the first time that loading MoS_2 on CdS enhanced significantly H_2 photoproduction by CdS, under visible light irradiation. The authors also found that CdS/MoS_2 presented higher H_2 production rates than CdS loaded with noble metals (including Pt), under the same reaction conditions[88]. Moreover, several CdS/MoS_2 nanocomposites with excellent photocatalytic H_2 production performances have also been developed. These systems usually involved CdS nanostructures (e.g.: nano -particles, -roads and -wires) loaded with MoS_2 nanosheets, which enhanced cadmium sulfide stability and catalytic performance[87,89–92].

Similarly, to Mo, cocatalysts W and Ni have also been loaded on CdS surface. In their follow-up work, Zong *et al.* hypothesized that since MoS_2 and WS_2 are both members of TMD compounds and have an extremely similar crystal structure, WS_2 could be a promising cocatalyst for H_2 evolution, which was verified due to its excellent catalytic performance towards H_2 formation[93]. Additionally, several reports describe the creation of CdS/WS_2 nanocomposites, mostly using WS_2 nanosheets loaded on CdS, for H_2 photoproduction[94–96]. Relatively to Ni, works involving CdS or CdS nanostructures (NPs and nanowires) conjugated with NiS nanoparticles have also been reported for H_2 evolution under visible light[97–100].

1.4. – Objective

The main goal of this work was the development of a new biophotocatalytic system, based on self-photosensitization of non-photosynthetic anaerobic bacteria with metal sulfide nanoparticles, for solar-hydrogen production. Thus, the construction of a new biohybrid system with a higher efficiency than the previously reported was intended, which involved the following steps:

1) Selection of best microorganism as biocatalyst for H_2 photoproduction:

For this purpose, four non-photosynthetic anaerobic microorganisms *Citrobacter freundii*, *Clostridium acetobutylicum*, *Desulfovibrio vulgaris* and *Desulfovibrio desulfuricans* were selected based in their potential for H_2 production.

2) Selection of best semiconductor as light-harvesting material for H_2 photoproduction

Monovalent (CdS) and CdS-binary nanocomposites (WS$_2$, MoS$_2$ and NiS$_2$) were studied as light-harvesting material

3) Immobilization of selected biohybrid system in calcium alginate beads
4) Development of a photocatalytic process for light-driven H_2 production

2

Chapter 2: Material and Methods

2.1. – Microorganisms and growth conditions

In this work different anaerobic bacteria were studied as biocatalyst for the creation of the photocatalytic system, namely two sulfate reducing bacteria (SRB) and three fermentative organisms (including *Escherichia coli*).

All flasks that contained the medium used for anaerobic growth, were previously purged with nitrogen (N_2) for at least 20 min and latter sealed and autoclaved, to achieve anaerobic conditions.

2.1.1. - Growth of sulfate reducing bacteria

The SRB used in this study were *Desulfovibrio desulfuricans* (ATCC 27774) and *Desulfovibrio vulgaris* Hildenborough (ATCC 29579). *D. desulfuricans* and *D. vulgaris* were grown anaerobically in medium Postgate C in presence of lactate, as carbon source and sulfate as electron acceptor. The composition of the medium Postgate C is described in **Table 2.1.** The SBR were grown at 37ºC for 20 h. An inoculum of 10 % (v/v) was used.

Table 2.1.- Composition of medium Postgate C.

Compound	g L^{-1}	Label
NH$_4$Cl	1	Scharlau
KH$_2$PO$_4$	0.5	Panreac
CaCl$_2$•2H$_2$O	0.06	Merck
MgCl$_2$•7H$_2$O	0.06	Roth
Yeast extract	1	Scharlau
FeSO$_4$•7H$_2$O	0.0071	Fluka
Trisodium citrate•2H$_2$O	0.3	Panreac
Ascorbic acid	0.1	Sigma
Sodium thioglycolate	0.1	Sigma
Sodium sulfate (17.6 mM)	2.5	Panreac
Sodium lactate (40 mM)	7.2 mL (from 5.6 M)	Panreac
Resazurin (160 µmol L^{-1})	1.6 mL (from 100 mg L^{-1})	Sigma
pH = 7.2 ± 0.2		

Resazurin is an anaerobic indicator which is colorless in the absence of O$_2$ and turns pink when it is in contact with oxygen (**Table 2.1**.).

2.1.2. - Growth of fermentative organisms

The fermentative organisms studied in this work were *Citrobacter freundii* (DSM 24394), *Clostridium acetobutylicum* (DSM 792) and the model organism *Escherichia coli* (NZY5α) (NZYTech).

C. freundii stored was grown aerobically in tryptic soy broth (TSB) medium (30 g L^{-1}) (Merck), overnight at 37 °C on a rotary shaker (150 rpm). *E. coli* was also cultivated under aerobic conditions for overnight at 37°C, 150 rpm, but in Luria-Bertani broth (LB) medium (25 g L^{-1}) (NZYTech).

C. acetobutylicum was grown anaerobically on Peptone Yeast Glucose (PYG) broth medium, at 37 °C for 24 h. The composition of medium PYG is illustrated in **Table 2.2.**

Table 2.2. - Composition of medium PYG.

Composition	g L^{-1}	Label
Tryptone	10	Biokar
Yeast extract	10	Scharlau
Salt solution[1]	40 mL	
Sodium thioglycolate	0.5	Sigma
L-cysteine (4.1 mM)	0.5	Roth
D-glucose (28 mM)	5	Sigma
Sodium sulfide (1 mM)	0.2	Panreac
Resazurin (160 µmol L^{-1})	1.6 mL (from 100 mg L^{-1})	Sigma
pH = 7		

[1] Salt solution constitution: $CaCl_2 \cdot 2H_2O$ (0.25 g L^{-1}), NaCl (10 g L^{-1}) (Sigma), $MgSO_4 \cdot 7H_2O$ (0.5 g L^{-1}) (Sigma), KH_2PO_4 (1g L^{-1}) (Panreac), K_2HPO_4 (1 g L^{-1}) (Panreac) and $NaHCO_3$ (10 g L^{-1}) (Alfa Aesar).

2.2. – Synthesis of biohybrid cells-semiconductor system

2.2.1 - Construction of biohybrid system with monovalent semiconductor (CdS)

To produce biologically the monovalent semiconductor cadmium sulfide, it is necessary to provide cadmium to the grown bacterial culture, that will react with the hydrogen sulfide (H_2S) generated by the bacteria, allowing the formation of CdS.

D. desulfuricans and *D. vulgaris* were grown in a specific medium to allow the production of biological CdS, designated by medium BioCdS. This medium was similar to medium Postgate C (**Table 2.1.**) except in: *i)* did not contain phosphate (KH_2PO_4), to prevent chemical precipitation of Cd as cadmium phosphate *ii)* had a slighter higher sulfate amount (20 mM instead of 17.6 mM present in medium Postgate C) and *iii)* medium BioCdS was supplement with two metal cofactors: 1 µM of nickel (as nickel chloride) (Sigma) and 1 µM of selenium (as sodium selenite solution) (Fluka). The pH of the medium was adjusted to 6.6±0.2, which allows the precipitation of cadmium as cadmium sulfide, since CdS is not soluble at a pH higher than 4[101].

Thus, SRB grown on Postgate C medium were used to inoculate 50 mL of medium BioCdS (10 % (v/v) of inoculum) and incubated at 37 °C for 17 h. In the end of the exponential phase, cadmium chloride ($CdCl_2$) (Fluka) was added slowly to the culture (to make sure that metal would be retain on cells). Then, the culture was incubated with cadmium for 3 h at 37 °C to assure that all Cd precipitated as cadmium sulfide. As a result, a biohybrid system is formed, constituted by the bacteria and the generated CdS.

C. freundii, *C. acetobutylicum* and *E. coli* followed an identical procedure of SRB bacteria to generate biologically CdS. *C. freundii* previously grown aerobically were used to inoculate an anaerobic flask containing 50 mL of medium denominated by Citro (**Table 2.3.**). Similarly, *E. coli* grown aerobically was transferred to 50 mL of anaerobic LB medium supplemented with L-glucose (27.8 mM) and L-cysteine (4.1 mM). *C. acetobutylicum* cultivated anaerobically were once again inoculated in 50 mL of medium PYG. All three bacteria were incubated at 37 °C in static conditions. Then, cadmium chloride was added to bacteria cultures and incubated with cells for 3 h at 37 °C.

C. freundii, *E. coli* and *C. acetobutylicum* use L-cysteine as sulfur source originating the hydrogen sulfide needed for CdS biogeneration.

Table 2.3. - Composition of medium Citro.

Composition	g L^{-1}	Label
Tryptone	5	Biokar
Yeast extract	5	Scharlau
Sodium thioglycolate	0.1	Sigma
Ascorbic Acid	0.1	Sigma
FeSO$_4$•7H$_2$O	0.0071	Fluka
L-cysteine (4.1 mM)	0.5	Roth
D-glucose (27.8 mM)	5	Sigma
MgSO$_4$7H$_2$O (2 mM sulfate)	0.5	Sigma
Resazurin (160 µmol L^{-1})	1.6 mL (from 100 mg L^{-1})	Sigma
pH = 7.4		

2.2.2. - Construction of biohybrid systems with divalent semiconductors

Several biohybrid systems were also constructed using the combination of CdS semiconductor with other metals (cocatalysts): molybdenum (Mo), tungsten (W) and nickel (Ni), resulting in the divalent semiconductors CdS-MoS$_2$, CdS-WS$_2$ and CdS-NiS, respectively.

Hence, CdCl$_2$ was added to bacteria culture followed by the addition of the second metal: Na$_2$MoO$_4$ (Carlo Erba), Na$_2$WO$_4$ (Fluka) or Cl$_2$Ni•6H$_2$O (Sigma), that was also added slowly to cells. The resulting biohybrid systems were incubated at 37ºC for 3 h.

2.3. – Photoproduction of H₂ by biohybrid system

The photocatalytic assays were performed anaerobically on 11 mL glass flask, with a working volume of 6.5 mL and magneto inside. These flasks were sealed with anaerobic stoppers and purged with nitrogen during 10 min. The assays were conducted using a photocatalytic solution composed by 20 mM Tris-HCl anaerobic buffer (pH=7.6) supplemented with HCl-cysteine (3.2 mM) (Merk) that acted as reducing agent and resazurin (0.8 µM) as anaerobic indicator. Additionally, HCl-cysteine (12.3 mM) (Merck) was added to the flasks as sacrificial electron donor (SED).

The photocatalytic assay initiated with the addition of the biohybrid system to the photocatalytic solution. Thus, 22.5 mL of the system was collected, washed with anaerobic 20 mM Tris-HCl buffer containing HCl-cysteine, centrifuged (5800 rpm, 10 min) and resuspended on the anaerobic buffer and added to the photocatalytic flask. The biohybrid system were then exposed to a light source. Headspace samples of the photocatalytic flasks were periodically collected to measure the hydrogen content.

The effect of Cd concentration (0.5 to 4 mM), presence of electron shuttle (0.5 mM of methyl viologen), sacrificial electron donor (0 to 28 mM of cysteine), concentration of cocatalysts (ranging from 0.001 to 1.5 mM) and light source (violet LEDs and solar simulator) was evaluated. Control experiments for H₂ production, were also carried out: *1)* inactivated biohybrid system irradiated with light, where cells were killed by autoclave (120 ºC, 30 min), *2)* biohybrid system under dark condition (where flasks were cover with aluminum paper to protect the system from light) and *3)* CdS-free cells irradiated with light.

Experiments were carried at least in triplicate and all values are expressed as means ± standard deviation.

2.4. – Characterization of light sources

The photocatalytic system was exposed to two different illumination sources: LEDs and a solar simulator.

Relatively to LEDs, the photocatalysis flasks were incubated on a glass vessel covered with aluminum paper that contained a circular violet LED inside. The vessel was place under stirring plate and at 4 ºC to maintain the temperature of reaction on 30 ºC (**Figure 2.1. A**). The two violet LEDs tested emitted visible light at λ= 445 nm, but with different irradiances: 0.042 mW cm^{-2} (**Figure 2.1. B**) and 3.6 mW cm^{-2} (**Figure 2.1. C**).
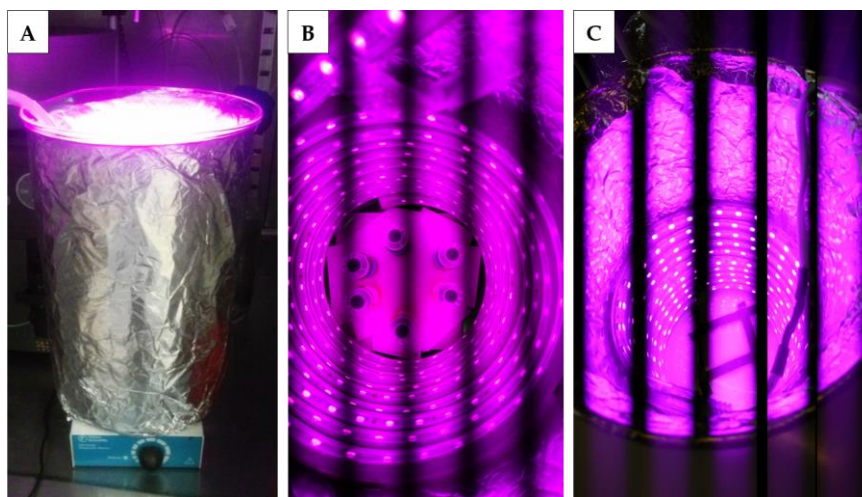
Figure 2.1. - LED as light source. Setup of LEDs for the photocatalytic experiments (**A**). The two violet LED sources with 0.042 mW cm^{-2} (**B**) and 3.6 mW cm^{-2} (**C**) of irradiance.

The solar simulator consisted of a 300 W Xenon lamp (Sirius-300P, Zolix) with an irradiance of 21 W cm^{-2} (200-450 nm). The flasks were stirred magnetically and the temperature was maintained at 25 ºC by a refrigerated bath (**Figure 2.2**).
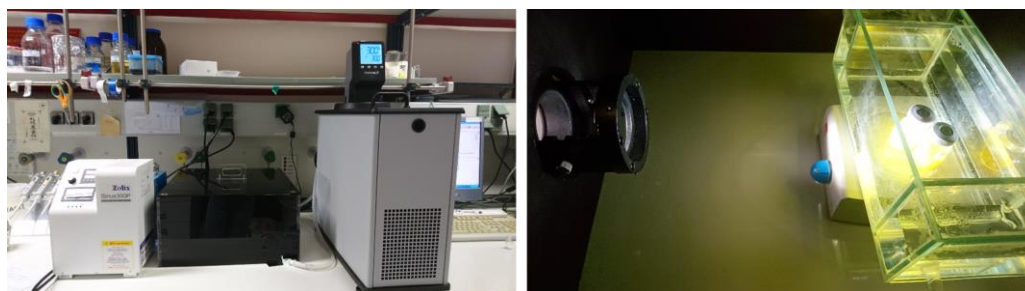
Figure 2.2. - The assay setup using the solar simulator as light source.

The energy supplied by the light source must be superior to the CdS band gap (E_g=2.4 eV), to allow electron conduction in the semiconductor[79]. The violet LEDs emit light at λ= 445 nm that corresponds to an energy value between 2.52 and 2.84 eV, which is enough to excite electron on CdS.

2.5. – Determination of hydrogenase activity of whole-cells

The hydrogenase activity of whole-cells was also determined, using the bacterial cells anaerobically grown as described in section *2.2.1.*

The assays were conducted on an anaerobic 11 mL vial. The reaction mix was constituted by 5 mL of Tris-HCl anaerobic buffer (50 mM, pH=7.6), 0.5 mL of methyl viologen (0.5 mM) and 0.5 mL of dithionite (5 mM). Dithionite is a reducing agent that will reduce the methyl viologen. The reduced MV transfers electrons to cells, allowing H_2 production. The assay started with the addition of cells (that were previously centrifuged at 4400 rpm for 10 min and resuspended in 0.5 mL of anaerobic buffer). Headspace samples were collected to measure the hydrogen content.

2.6. – Characterization of biohybrid systems

The characterization of the biohybrid systems was performed by scanning electron microscopy and energy dispersive spectroscopy (SEM-EDS).

2.6.1. - Preparation of the biohybrid system samples for SEM-EDS

Five mL of the biohybrid systems were collected, centrifuged (4400 rpm, 10 min) and washed with Tris-HCl buffer (20 mM, pH= 7.2). This step was repeated for 2 times. The system was then fixed with 1 mL of fixative solution (constituted by 2.5 % (w/v) glutaraldehyde and 2 % (w/v) formaldehyde in Tris-HCl buffer) and incubated at 4 °C overnight. To remove the fixative solution, the biosystem was washed and resuspended in 1 mL of buffer and incubated for 10 min at room temperature (this step was repeated for 3 times). Subsequently, the systems were

fixed with 1 % (w/v) osmium, for 1 h at -4 °C and washed with Tris-HCl buffer followed by room temperature incubation, as described above. The samples were dehydrated through 1 mL of graded ethanol series (30, 50, 75, 90, 100 % of ethanol (v/v)) for 10 min in each solution. Samples were frozen in liquid nitrogen and lyophilized.

2.6.2. - SEM-EDS of biohybrid system

Photosystems samples were placed onto an Al stub using double-sided carbon tape. A thin film of Au/Pd was deposited on their surface using a Quorum Technologies model Q150T ES. The samples were then viewed with a FEG-SEM JEOL JSM7001F and for SEM-EDS a light elements Si (Li) detector by Oxford, model INCA250, was used.

2.7. – Immobilization of biophotocatalytic system

The immobilization of biohybrid system was also conducted by entrapment in calcium alginate beads.

The biohybrid system (22 mL) was recovered by centrifugation (4400 rpm, 10 min) and resuspended in 2 mL of anaerobic water. Then, 20 g L^{-1} of sodium alginate (Sigma), was added slowly to the system. Subsequently, biohybrid-sodium alginate suspension was added by drop by drop using a syringe, to a calcium chloride solution (0.5 M) (Panreac) for cross-linking to form spherical biohybrid-calcium alginate beads (**Figure 2.3.**)[102–104]. Beads stayed for 15 min in $CaCl_2$ solution for curing. The cured beads were collected and used in the photosynthetic assays.
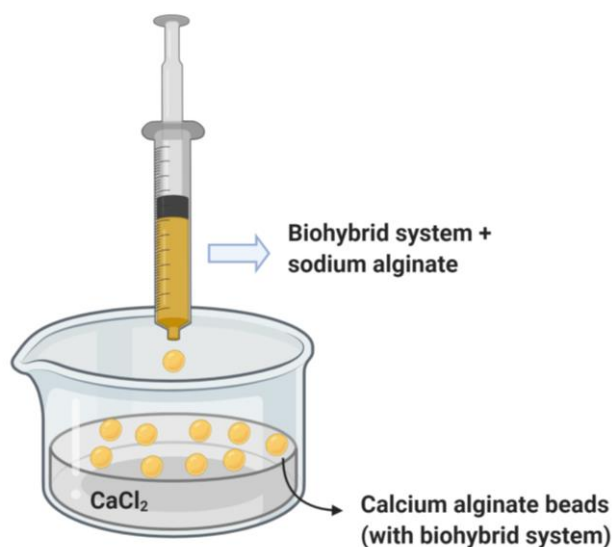
Figure 2.3. – Immobilization of biohybrid system in calcium alginate beads (setup). Created with BioRender.com.

2.8. – Photoreactor for H_2 production

A batch reactor for H_2 production was developed using the best biohybrid system.

Hydrogen production was carried out in a designed glass column reactor (inner diameter= 5.5 cm, height= 35 cm and volume= 750 mL) with violet LEDs strips (λ= 445 nm, 3.6 mW cm^{-2}, (**Figure 2.1. C**)) attached to the vessel exterior (**Figure 2.4.**).

The reactor operated with a working volume of 400 mL, at 40 °C and was magnetically stirred (**Figure 2.4.**). Thus, 350 mL Tris-HCl anaerobic buffer with HCl-cysteine was added to the reactor and purged with N_2, to assure anaerobic conditions. 2 L of biohybrid system was concentrated in 50 mL of anaerobic buffer and added to the reactor. The electron shuttle (0.5 mM of MV) and sacrificial electron donor (30 mM of cysteine) were also added to the reactors. Headspace samples were periodically collected to measure the H_2 content.
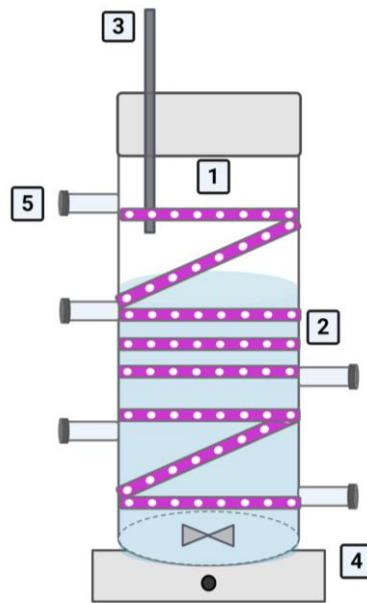
Figure 2.4. - Schematic illustration of batch reactor. Bioreactor (**1**), LEDs (**2**), temperature sensor (**3**), magnetic stirred and stir plate (**4**), sample ports (**5**). Created with Biorender.com.

2.9. – Analytical methods

Cell growth was monitored by measuring optical density at 600 nm (OD_{600}) with Ultrospec 10 Cell Density Meter (Biochrom). Biomass were determined by measuring dry cell weight (dcw), obtained at overnight incubation at 60ºC, and correlated with OD_{600} values. One-unit value of OD_{600} corresponded to 0.31 g_{dcw} L^{-1} for both *D. desulfuricans* and *D. vulgaris*, 0.36 g_{dcw} L^{-1} for *C. freundii* and 0.34 g_{dcw} L^{-1} for *E. coli*.

The H_2 content in the headspace of the photocatalytic flaks was determined using a Trace GC 2000 gas chromatograph (Thermo Corporation) equipped with a MolSieve 5A 80/100 column (Altech) and a thermal conductivity detector (TCD). Nitrogen was used as carrier gas at a flow rate of 10 mL min^{-1}. To study H_2 production, a H_2 calibration curve was traced (**Figure A1., Table A1.**). For this purpose, a photocatalytic flask with a working volume of 6.5 mL was injected successively with a known volume of H_2 (from 20 to 2000 µL) and the

correspondent GC areas were obtained. The equation of real gases was used to determinate the number of moles of H_2:

$$PV = nRT$$

where P = 1 atm, R=0.082057 atm•L•mol^{-1}•k^{-1}, T= 298 K and V was the H_2 volume injected (µL) in the photocatalytic flask.

Thus, the resulting calibration curve enable the obtention of the following equation (**Figure A1.**, **Table A1.**):

$$H_2(\mu mol) = 4 \times 10^{-6} \times GC\ Area, \qquad R^2 = 0.998$$

To determine the specific hydrogen production rate (µmol g$_{dcw}$$^{-1}$ h^{-1}), a linear regression was trace on a plot with H_2 production (µmol g$_{dcw}$$^{-1}$) per time (h), where the slop was the specific H_2 production rate. The same method was applied to calculate the whole-cell hydrogenases activities (**Figure A2.**).

Hydrogen production and apparent quantum yields (AQY) were determined based on the photocatalytic reaction of H_2 production by the biohybrid systems (**Equation 2.1.**):

$$2\ Cysteine + 2\ hv \xrightarrow{Bacterium-CdS} Cystine + H_2 \quad (\textbf{Equation 2.1.})$$
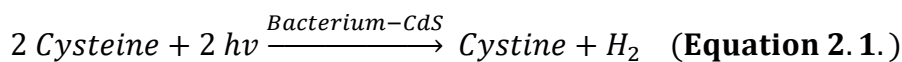
where photons are represents by *hv.*

Thus, the H_2 production yield was calculated by the following equation (**Equation 2.2.**):

$$H_2\ Yield\ (\%) = (\ H_2\ /(\frac{Cysteine}{2})) \times 100 \qquad (\textbf{Equation 2.2.})$$

The apparent quantum yield (AQY) was determined using the **Equation 2.3**[47,50]:

$$AQY\ (\%) = \frac{number\ of\ electroes\ used\ to\ produce\ H_2}{number\ of\ incident\ photons} \times 100$$

$$AQY\ (\%) = \frac{2 \times C_{H2} \times N_A}{\frac{P \times A \times t \times \lambda}{h \times c}} \times 100 \qquad (\textbf{Equation 2.3.})$$

where C_{H2} (in moles) is the H_2 produced during the irradiation time (t, in seconds), N_A is Avogadro's number (6.022×10^{23}), P is the power density of energy source (W cm^{-2}), A is the irradiation area (cm^2), λ is the wavelength of light (m), h is Planck constant (6.63×10^{-34} J s) and c is speed of light (3×10^8 m s^{-1}). The irradiation area (A) was assumed to be the entire surface of the flask (16.6 cm^2), even though there was scattering and reflection losses due to the curved sidewalls of the tubular reaction flasks.

Chapter 3: Results and Discussion

The design of a biophotocatalytic system for hydrogen production was carried out. The system was composed by non-photosynthetic anaerobic bacteria as biocatalyst and self-produced cadmium sulfide nanoparticles (CdS). The CdS precipitates on the bacterial cell surface acting as a semiconductor to drive electrons from the energy source (visible light) to the bacteria, culminating in hydrogen production (**Figure 3.1.**).

Furthermore, the system also included a sacrificial electron donor (SED), that donates electrons (reduction) to quench the *hole*s generated by CdS after photon absorption. An electron transfer mediator, methyl viologen (MV) may be used to facilitate the electron transfer to the cell's hydrogenases (**Figure 3.1.**).
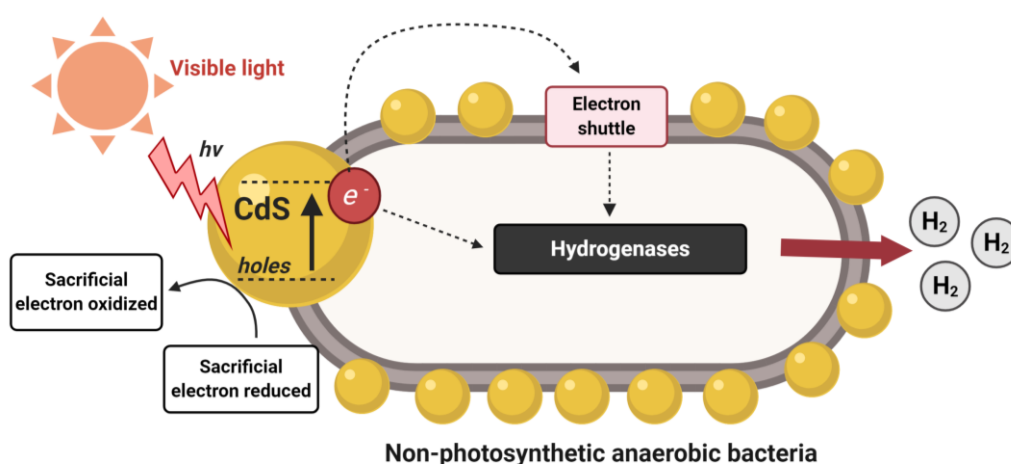
Figure 3.1. - Schematic representation of the biophotocatalytic system for H_2 production from visible light. The system is composed by non-photosynthetic anaerobic bacteria (biocatalyst) and CdS biologically produced (semiconductor). Created with Biorender.com.

Cadmium sulfide is considered one of the most prominent semiconductors due to its excellent photocatalytic properties and visible-light response, thereby making CdS a suitable light-harvesting material for the presented system[79,105].

Sacrificial electron donors are molecules that are oxidized in the photocatalytic process, thus filling the electron-*holes* in the semiconductor[106,107]. Hence, SED not only enhances the semiconductor stability (by suppressing photocorrosion caused by the *holes*), but also prevents the recombination of the photogenerated electron-*holes*. As a result, it allows a more efficient electron transfer from semiconductor to the catalyst[107–109]. These electron donors have to fulfill the following 2 criteria: *1)* to have an appropriate electron potential (that has to be inferior to the semiconductors potential) and *2)* be irreversibly oxidized into an inert molecule (that does not interfere with the electron transfer process)[106]. Cysteine is an aminoacid with a thiol side chain that confers it high reactivity[110]. On the other hand, cystine is the oxidation product of two cysteine molecules (**Equation 3.1.**)[111].

$$2\ cysteine\ \rightarrow\ cystine\ +\ 2\ H^+ +\ +\ 2\ e^-\quad (\mathbf{Equation\ 3.1.})$$
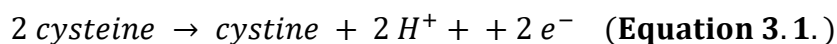
The exact value of standard oxidation-reduction potential of cystine/cysteine is challenging to calculate (due to thiol group reactivity), and two values are proposed in the literature, namely -0.22 V and -0.34 V, which were determined by different methods[111,112]. Nevertheless, the E_{VB} of CdS is 1.90 eV, which is higher than the E_0' cystine/cysteine, thus cysteine can be oxidized by the *holes* in CdS semiconductor[113]. Therefore, HCl-cysteine was used as sacrificial electron donor in the proposed biohybrid system.

Electron shuttles are organic molecules that can undergo reversible redox reactions, thereby having the ability to act as electron carriers[114,115]. Viologens are di-quarternized 4,4'-bipyridyl salts that present unique properties, particularly: three reversible and stable redox states, efficient electron-accepting capability and distinct color changes between viologens species[116–118]. Methyl viologen (MV) is one of the most studied viologen derivates. Therefore, MV^{2+} (the colorless di-cation specie) can undergo two stable and reversible reduction reactions,

resulting in MV$^{\bullet+}$ (a radical cation with an intense violet blue color) and MV formation (the neutral specie that is yellow-brown colored) (**Figure 3.2**)[116–118]. MV^{2+} has a pH-independent one electron reduction potential (E$^{'}_0$=-440 mV vs. normal hydrogen electrode, NHE), stable and long-lived radicals and is also soluble in water[119,120].
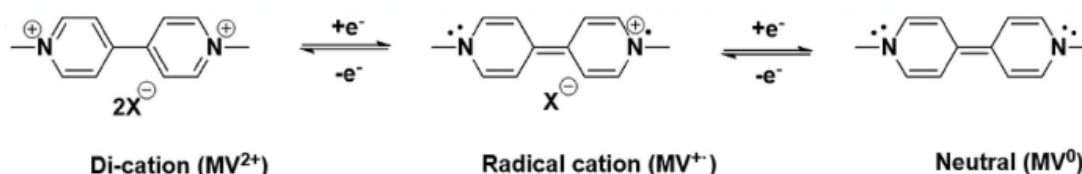
Figure 3.2. -The three reversible redox states of methyl viologen (MV).[116]

Thus, MV was used as electron shuttle in the biohybrid system. The MV^{2+} can receive electrons from the semiconductor, whereas MV$^{\bullet+}$ can further transfer the electrons to the cells[119]. As a result, methyl viologen can accelerate the electron transfer of CdS NPs to cell's hydrogenases, increasing the efficiency of H$_2$ production by the photocatalytic system. This electron transfer is possible because the MV redox potential (-440 mV) is lower than the redox potential of hydrogenases (-414 mV), allowing MV to supply electrons for the H$_2$ production (**Equation 3.2., Equation 1.1.**)[20,119].

$$MV \rightarrow MV^{2+} + 2e^- \qquad E_0 = -440\ mV \qquad (\textbf{Equation 3.2.})$$

$$2\,H^+ + 2e^- \rightarrow H_2 \qquad E_0 = -414\ mV \qquad (\textbf{Equation 1.1.})$$
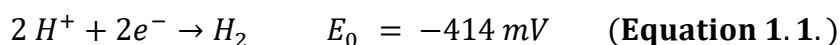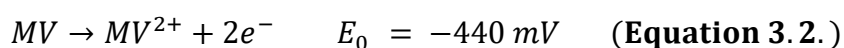
3.1. – Selection of best biocatalyst for H$_2$ photoproduction

The biocatalyst required for the biohybrid system must fulfill 2 criteria: *1)* be able to produce H$_2$ and *2)* present the ability to not only synthesize cadmium sulfide NPs, but also accept electrons from the semiconductor. Thus, 4 microorganisms were considered for biocatalysts: the fermentative organisms

Citrobacter freundii and *Clostridium acetobutylicum* and the sulfate reducing bacteria *Desulfovibrio vulgaris* and *Desulfovibrio desulfuricans*.

The optimal conditions for H_2 production for each system was determined and compared between systems, to select the best biocatalyst for H_2 photoproduction. Moreover, the performance of these biohybrid systems were further compared with the model organism *Escherichia coli*.

The photocatalytic assays were performed under LEDs light (with 0.042 mW cm^{-2} of irradiance).

3.1.1.- Biohybrid Citrobacter freundii-CdS system

3.1.1.1. - Creation of Citrobacter freundii-CdS system

The effective synthesis of CdS by *C. freundii* in the presence of 1 mM of Cd was demonstrated by the change of medium color that becomes yellowish after Cd addition, which it is an indicative of CdS formation (CdS presents a yellow color[37]) (**Figure 3.3**.). The complete removal of Cd from solution was confirmed by ICP analysis.
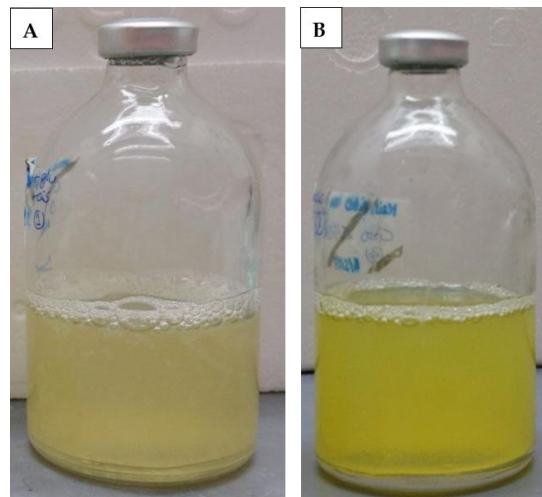
Figure 3.3. - Difference of color in medium inoculated with *Citrobacter freundii*, in absence of Cd (**A**) and with 3 h of incubation with 1 mM of Cd (**B**).

The SEM images showed the presence of nanoparticles on the *C. freundii* surface whereas in control cells (grown *C. freundii* without the addition of Cd), no precipitate was observed (**Figure 3.4 A, B.**). SEM-EDS proved that the nanoparticles were composed by cadmium and sulfur, proving that cadmium precipitated as cadmium sulfide (**Figure 3.4 C.**). The metals used in sample preparation (Os, Au and Pd) were also detected (**Figure 3.4. C.**).

The CdS precipitates in *C. freundii* cells formed large extracellular aggregates, that were not uniformly distributed between cells (**Figure 3.4. B.**). These results demonstrated the effective creation of *C. freundii*-CdS system.
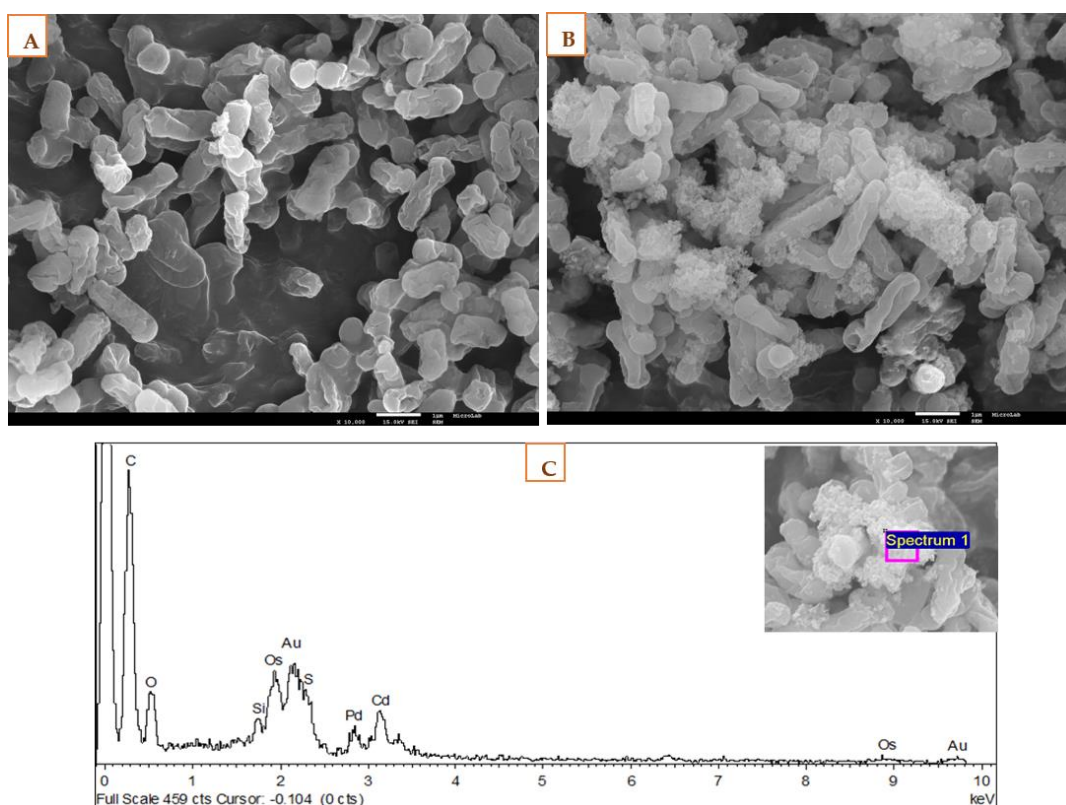
Figure 3.4.- Characterization of *Citrobacter freundii*-CdS. SEM images of *Citrobacter freundii* (**A**) and *Citrobacter freundii*-CdS biohybrid (**B**). EDS analysis of precipitated nanoparticles (**C**). The inset image shows the area where it was performed EDS.

3.1.1.2. - H$_2$ production profile of Citrobacter freundii-CdS system

To assess H$_2$ production by *C. freundii* -CdS system a series of photocatalytic assays were performed to determine the optimal conditions, to obtain the highest H$_2$ production.

It was observed that the *Citrobacter freundii*-CdS system in presence of MV was able to produce 5.4±1.3 µmol of H$_2$ after 143 h of light exposure, with a specific H$_2$ production rate of 7.8 µmol g_{dcw}^{-1} h^{-1} (**Figure 3.5.**).

Control experiments, in presence of MV, were also carried out to confirm H$_2$ production by biohybrid system. As showed in **Figure 3.5.**, H$_2$ production was not detected under dark conditions and with *C. freundii* without the self-produced CdS. However, inactivated cells-CdS system presented a minimal H$_2$ production of 0.4±0.1 µmol of H$_2$ after 143 h (**Figure 3.5.**). Cadmium sulfide has an intrinsic photocatalytic H$_2$-production activity, which can explain the generation of H$_2$ when cells were inactivated[79,121,122].
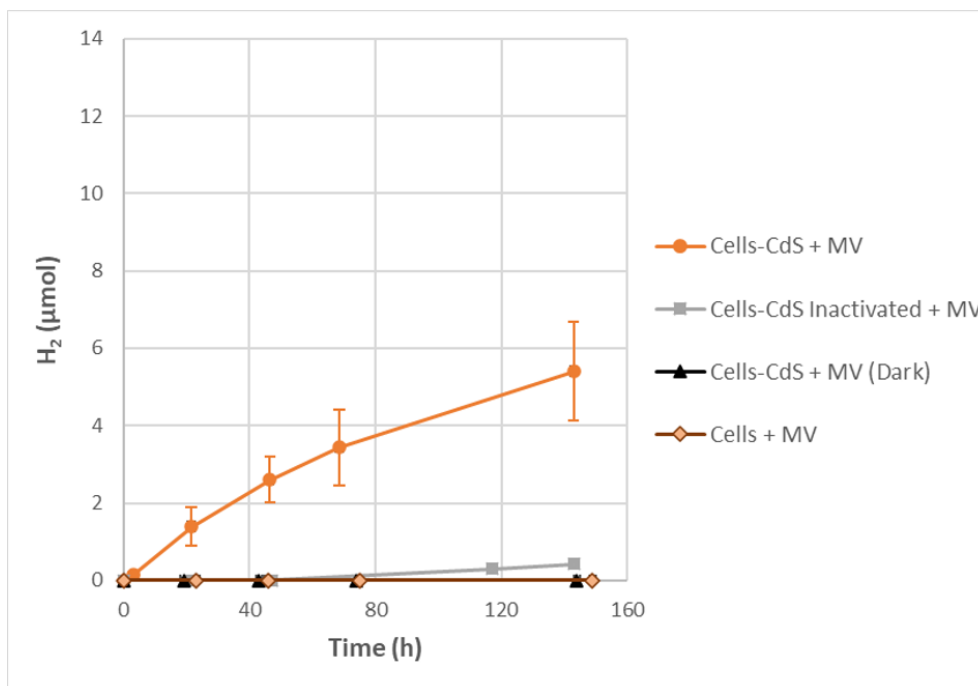
Figure 3.5. - Hydrogen photoproduction profile by *Citrobacter freundii*-CdS and its respective controls. Error bars indicate the standard deviations of the average values.

Hence, these experiments confirmed that H_2 production is only possible in the presence of *Citrobacter freundii* and self-produced CdS nanoparticles when the system was exposed to a light source.

3.1.1.3. - Effect of Cd concentration in H_2 production by Citrobacter freundii-CdS system

To investigate the impact of cadmium concentration on H_2 production, different Cd concentrations (from 0.5 to 4 mM) were used to synthetize the *C. freundii* biohybrids (**Figure 3.6.**).

The H_2 production of biohybrids constructed with concentrations from 0.5 to 3 mM of Cd were similar (~3.5 µmol), whereas with 4 mM of Cd the H_2 generated decreased (**Figure 3.6.**). Higher Cd concentration could be toxic to cells[123], decreasing the biocatalyst activity, leading consequently to a lower H_2 production.
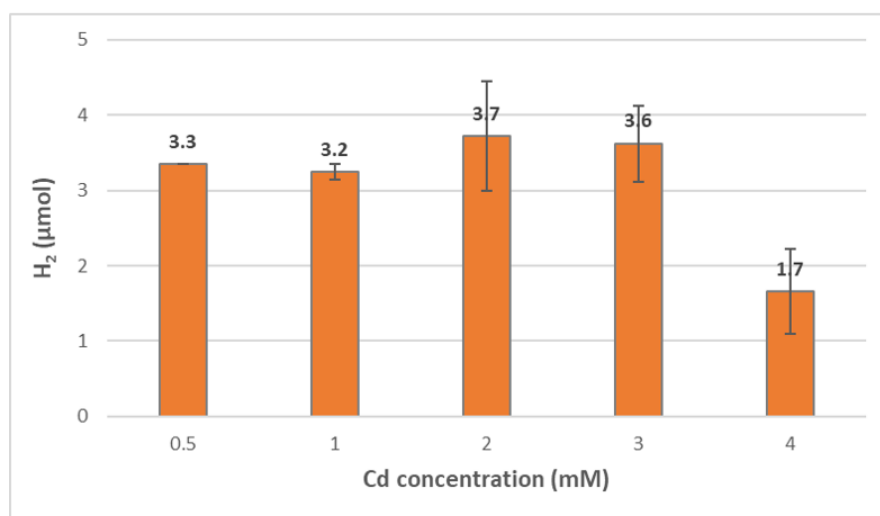
Figure 3.6. - Effect of Cd concentration on H_2 production by *Citrobacter freundii*-CdS. Data from 44 h. The error bars indicate standard deviation of the average values.

Thus, Cd concentration does not seem to have a pronounced effect on H_2 production performance by the *C. freundii*-CdS system, except when employing higher Cd concentrations (>3 mM).

3.1.1.4. - Effect of electron shuttle (MV) in H_2 production by Citrobacter freundii-CdS system

To study the influence of electron mediator in H_2 production performance of *C. freundii*-CdS, photocatalytic assays in the presence and absence of MV were carried out. Photosystem was constructed using 1 mM of Cd (**Figure 3.7.**).

C. freundii-CdS system presented a higher H_2 production in the presence of MV (5.4±1.3 µmol) than in absence of the electron shuttle (2.1±0.5 µmol), after 142 h of light irradiation (**Figure 3.7. A.**). The specific H_2 production rate of biohybrid system was 7.8 and 1.8 µmol g_{dcw}^{-1} h^{-1}, with and without MV, respectively. A higher photocatalytic activity in the presence of electron mediator MV, was also verified for the other developed biohybrid systems[19,33,34,52]. Since the role of MV in this system is to facilitate electron transfer between semiconductor to cell hydrogenases, the enhancement of H_2 performance in the presence of this electron shuttle is expected.
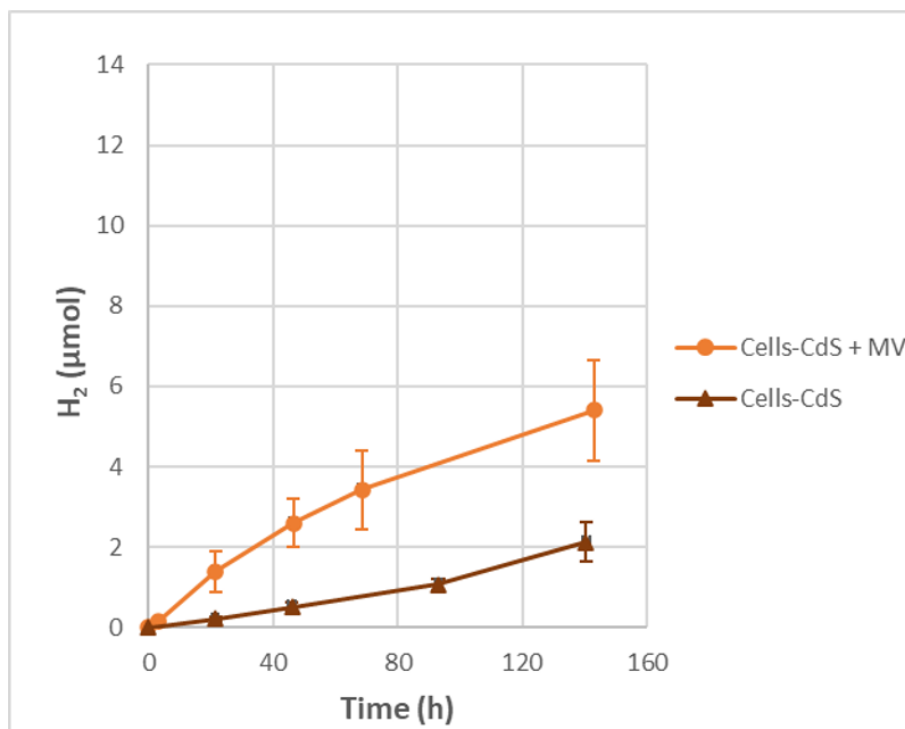
Figure 3.7. - Effect of MV in H_2 production by *Citrobacter freundii*-CdS system. The error bars indicate the standard deviations of the average values.

Therefore, the presence of MV enhances H$_2$ production performance of *C. freundii*-CdS system.

3.1.2. - Biohybrid Clostridium acetobutylicum-CdS system

Although *C. acetobutylicum* could present a great potential as biocatalyst for the creation of biohybrid system, we were not able to biologically produce CdS particles with this microorganism, which are required to build the photocatalytic system. As illustrated in **Figure 3.8.**, the medium did not turn the characteristic yellow color of CdS, after the addition of 1 mM of Cd. Hence, it was hypothesized that *C. acetobutylicum* did not generated enough sulfide to precipitate CdS.
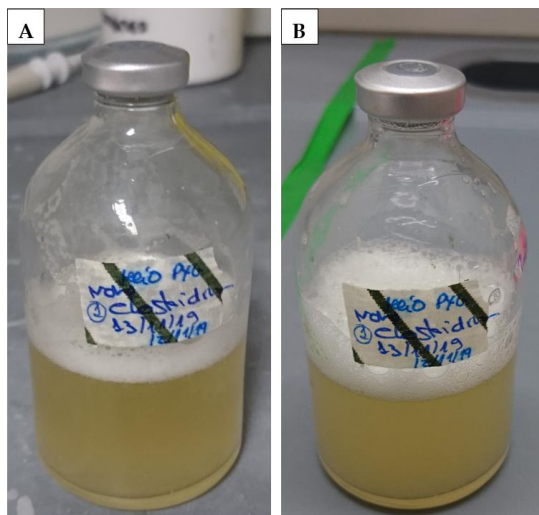
Figure 3.8. - Color of medium inoculated with *Clostridium acetobutylicum* before (**A**) and after (**B**) the addition of 1 mM of Cd.

Thus, the construction of a biohybrid system for H$_2$ production using *Clostridium acetobutylicum* as biocatalyst was not attained.

3.1.3. - Biohybrid Desulfovibrio vulgaris-CdS system

3.1.3.1. - Creation of Desulfovibrio vulgaris-CdS system

As showed in **Figure 3.9.**, medium become yellowish after the addition of 1 mM of Cd, thereby demonstrating the ability of *D. vulgaris* to biologically synthetize CdS.
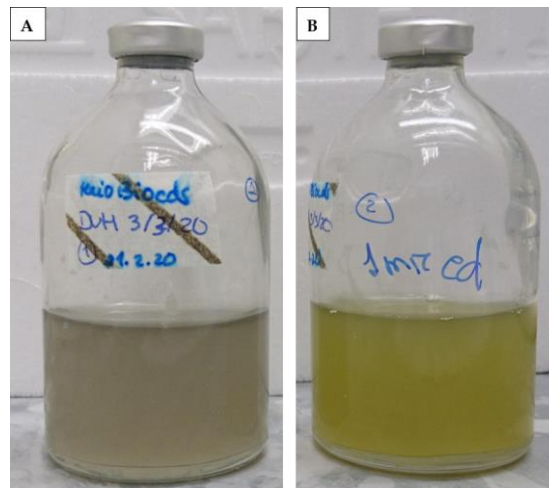
Figure 3.9. - Difference of color in medium inoculated with *Desulfovibrio vulgaris*, in absence of Cd (**A**) and with 3 h of incubation with 1 mM of Cd (**B**).

The characterization by SEM-EDS of the developed *Desulfovibrio vulgaris*-CdS biohybrid system was carried out (**Figure 3.10**). In grown *D. vulgaris* where Cd was not introduced (control cells), it was not detected any metal precipitates (**Figure 3.10. A**). Conversely, when Cd was added to bacteria, nanoparticles were generated on *D. vulgaris* cells surface (**Figure 3.10 B.**). These NPs were in fact CdS precipitates, as demonstrated by EDS analysis (**Figure 3.10 C.**) and seems to be evenly distributed between all bacterial cells (**Figure 3.10 B.**).
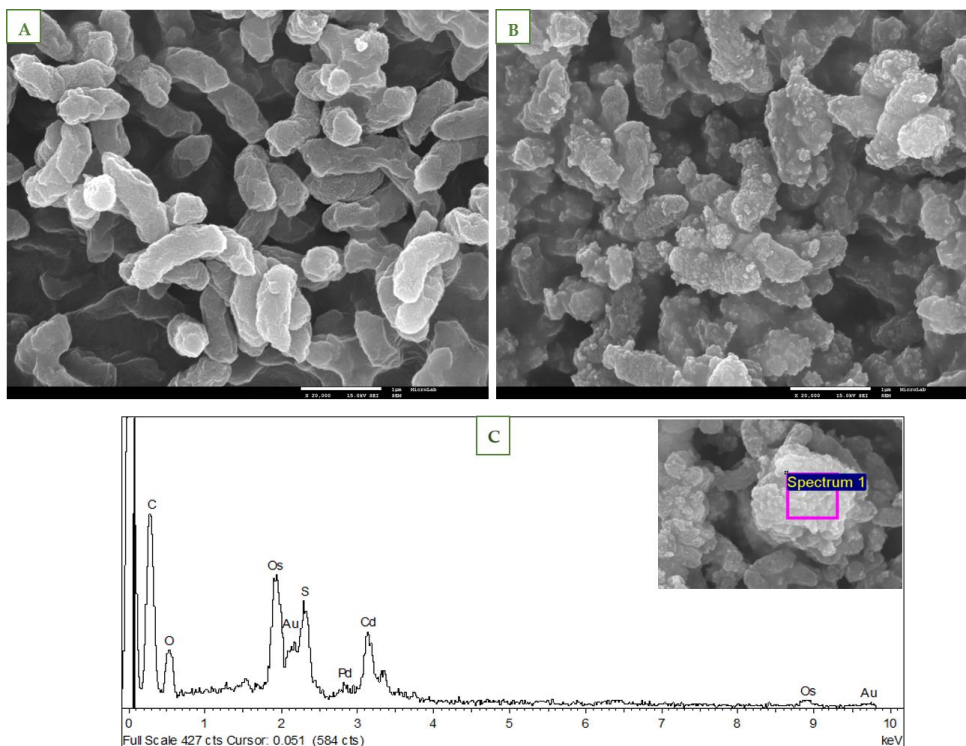
Figure 3.10.- Characterization of *Desulfovibrio vulgaris*-CdS. SEM images of *Desulfovibrio vulgaris* (**A**) and *Desulfovibrio vulgaris*-CdS biohybrid (**B**). EDS analysis of precipitated nanoparticles (**C**). The inset image shows the area where it was performed EDS.

Therefore, it has been proven that *D. vulgaris* can self-produce the CdS nanoparticles require for biohybrid system construction (**Figure 3.10.**). However, *D. vulgaris*-CdS system constructed with 1 mM of Cd in presence of MV presented a residual H_2 production (1.6±0.8 µmol) after 137 h of light exposure (**Figure 3.11.**).
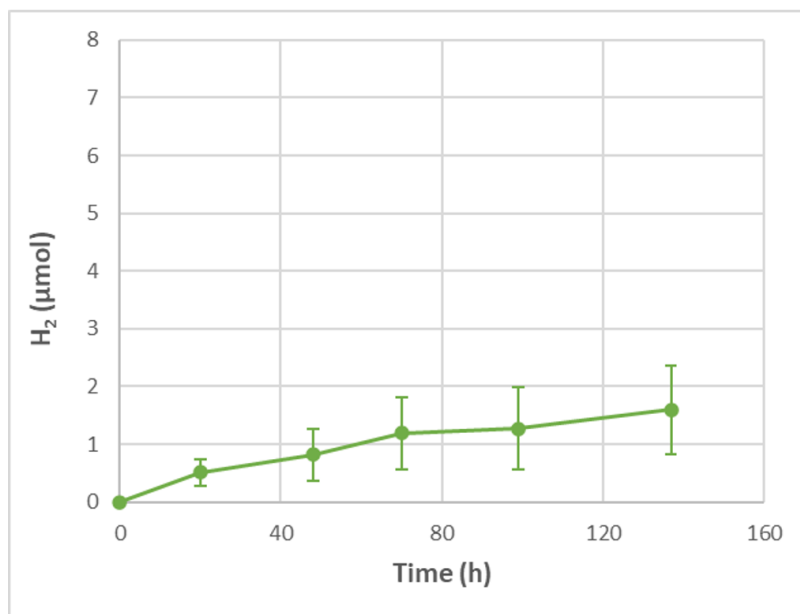
Figure 3.11. - Hydrogen photoproduction of *Desulfovibrio vulgaris*-CdS (1 mM of Cd, in presence of MV). Error bars indicate the standard deviations of the average values.

3.1.3.2. - Effect of Cd concentration in H_2 production by Desulfovibrio vulgaris-CdS system

Since H_2 production by *D. vulgaris*-CdS were substantially low with 1 mM of Cd (**Figure 3.11.**), it was hypothesized that the cadmium concentration used was not the most suitable and the optimal Cd concentration to construct this biohybrid. Therefore, different Cd concentrations were tested to create *D. vulgaris*-CdS system namely 0.5, 1, 2, 3 and 4 mM of Cd, in the presence of MV (**Figure 3.12.**).

Overall, the biohybrid systems still presented a very low H_2 production, regardless Cd concentration employed (**Figure 3.12.**). Nevertheless, *D. vulgaris*-CdS constructed with 3 mM of Cd generated 1.6±0.3 µmol of H_2 after 44 h of irradiation, that was superior to systems created with the remaining Cd concentrations (where all produced less than 1 µmol of H_2) (**Figure 3.12.**).
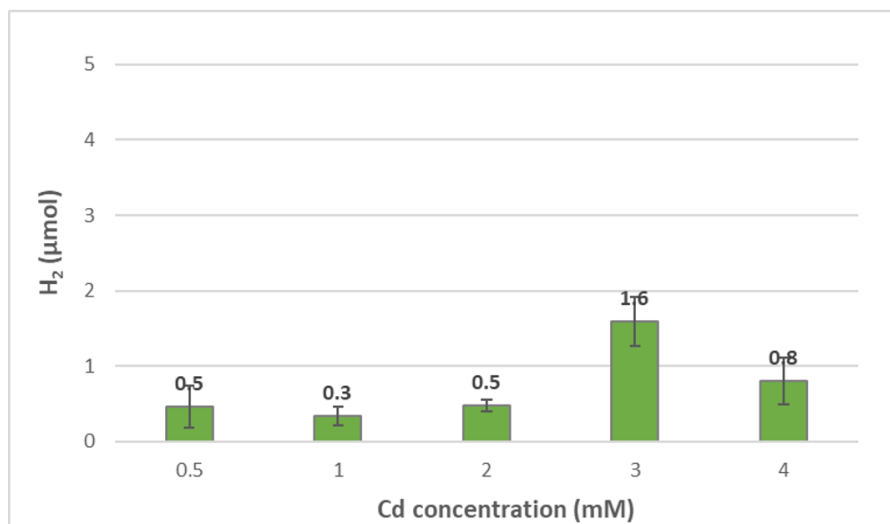
Figure 3.12. - Effect of Cd concentration on H_2 production by *Desulfovibrio vulgaris*-CdS. Data from 44 h. The error bars indicate standard deviation of the average values.

Therefore, the optimal Cd concentration determined for *D. vulgaris*-CdS system was 3 mM of Cd.

3.1.3.3. - Effect of electron shuttle in H_2 production by Desulfovibrio vulgaris-CdS system

The influence of electron mediator in H_2 production by *D. vulgaris*-CdS was investigated. Thus, photocatalytic assays were performed in the presence and absence of MV. Biohybrid was constructed using 3 mM of Cd (**Figure 3.13.**).

Interestingly, *D. vulgaris*-CdS had a higher H_2 production without MV (9.9±1.2 μmol) than with electron shuttle (2.4±0.9 μmol), after 141 h of LEDs light exposure (**Figure 3.13.**). The specific H_2 production rate in presence and absence of MV of biohybrid was 2.1 and 9.2 μmol $g_{dcw}^{-1}h^{-1}$, respectively.
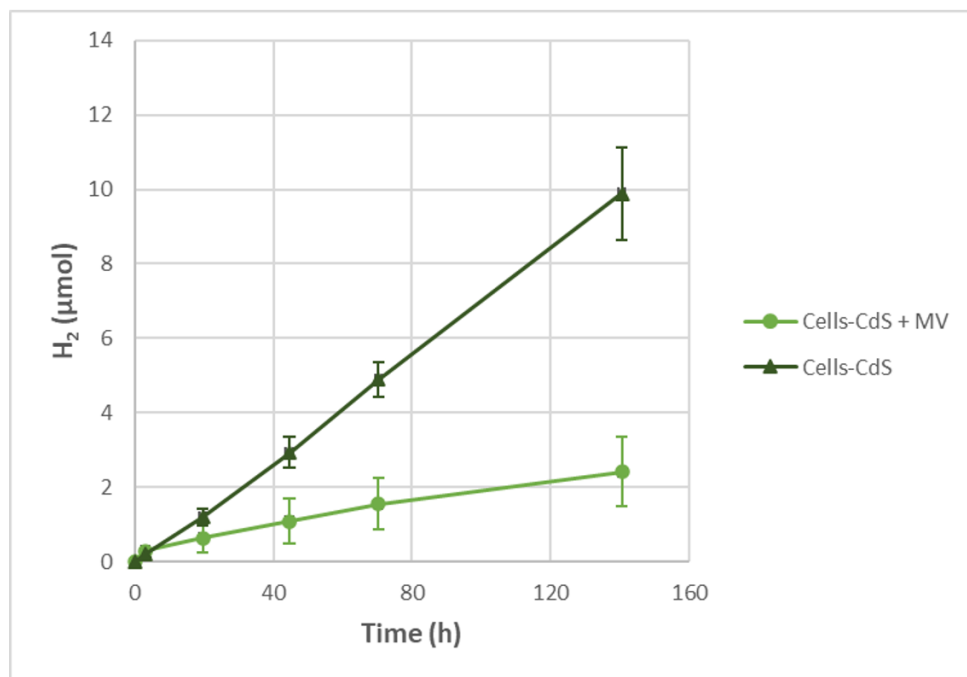
Figure 3.13. - Effect of MV in H_2 production by *Desulfovibrio vulgaris*-CdS system. The error bars indicate the standard deviations of the average values.

As aforementioned, electron shuttle assists the electron transfer process between CdS and cell hydrogenases. Therefore, MV was likely to present one of the following effects: *i)* enhance H_2 photoproduction, or *ii)* have a neutral impact on biohybrid performance. Thus, if MV presented a neutral impact it would be expected that *D. vulgaris*-CdS system with and without MV would have the same H_2 production profile, contrarily to the results obtained (**Figure 3.13.**). Further studies should be performed to assess *D. vulgaris*-CdS behavior towards electron mediator MV.

3.1.4. - Biohybrid Desulfovibrio desulfuricans-CdS system

3.1.4.1. - Creation of Desulfovibrio desulfuricans-CdS system

The synthesis of CdS by *Desulfovibrio desulfuricans* was obtained in the presence of 1 mM of Cd, as showed in **Figure 3.14.**, by the color change of medium to yellow, after the addition of Cd.
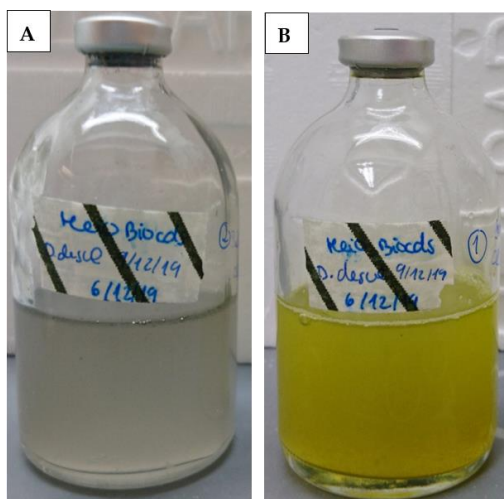
Figure 3.14. - Difference of color in medium inoculated with *Desulfovibrio desulfuricans*, in absence of Cd (**A**) and with 3 h of incubation with 1 mM of Cd (**B**).


SEM images demonstrated the precipitation of nanoparticles on *D. desulfuricans* cell surface, in presence of Cd (**Figure 3.15. B**). On contrary, in grown *D. desulfuricans* where cadmium was not added (control cells), SEM image did not reveal any precipitate (**Figure 3.15. A**). EDS analysis showed that the nanoparticles were composed by cadmium and sulfur, thereby proving that Cd precipitated in form of cadmium sulfide (**Figure 3.15. C**). The CdS nanoparticles forms agglomerates in cells surface of *D. desulfuricans* and it seems to be more concentrated in some cells compared with others (**Figure 3.15. B**). Therefore, these results showed the effective construction of *D. desulfuricans*-CdS system.
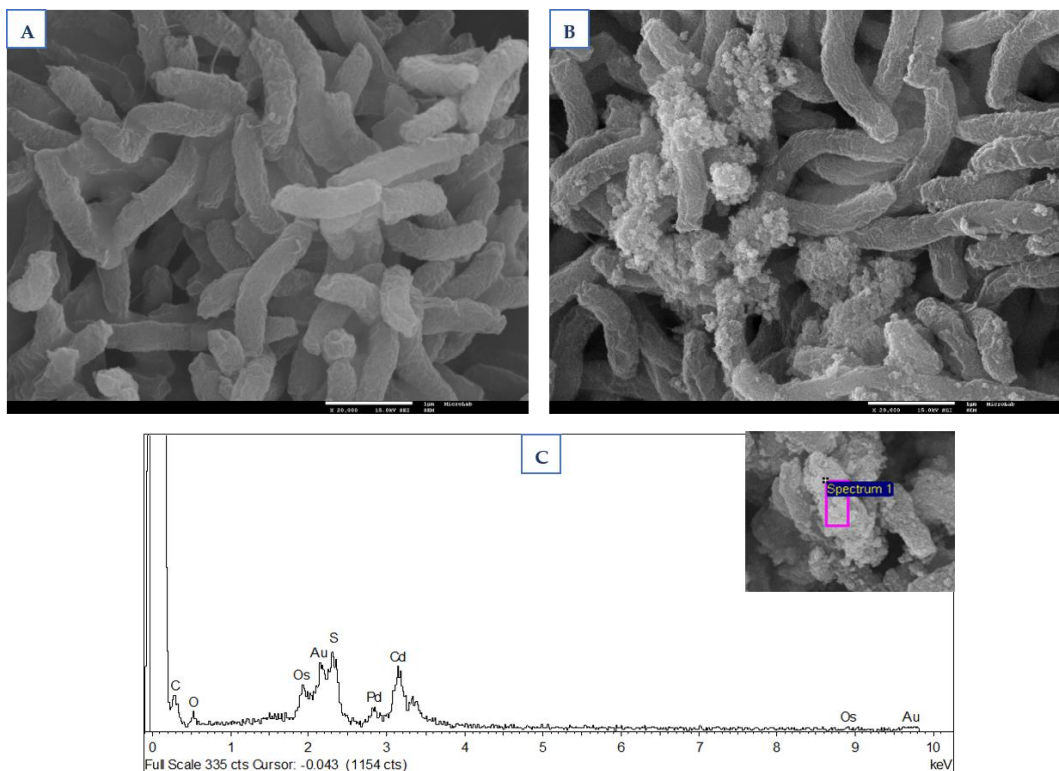
Figure 3.15.- Characterization of *Desulfovibrio desulfuricans*-CdS. SEM images of *Desulfovibrio desulfuricans* (**A**) and *Desulfovibrio desulfuricans*-CdS biohybrid (**B**). EDS analysis of precipitated nanoparticles (**C**). The inset image shows the area where it was performed EDS.

3.1.4.2. - H$_2$ production profile of Desulfovibrio desulfuricans-CdS system

To study H$_2$ production by *D. desulfuricans*-CdS system, several photocatalytic assays and control experiments were performed, in presence of MV.

The system *D. desulfuricans*-CdS/MV was able to produce 45.2±1.2 μmol of H$_2$ after 120 h of light exposure, with a specific H$_2$ production rate of 131 μmol g$_{dcw}^{-1}$ h^{-1} (**Figure 3.16.**).

Moreover, H_2 production was not detected under dark conditions and with *D. desulfuricans* without the biologically synthetized CdS semiconductor (**Figure 3.16.**). However, inactivated *D. desulfuricans*-CdS system had a slight H_2 production (0.5±0.2 µmol) after 120 h, similarly to what found for *C. freundii*-CdS system, that is probably due to intrinsic CdS photocatalytic activity (**Figure 3.16.**).
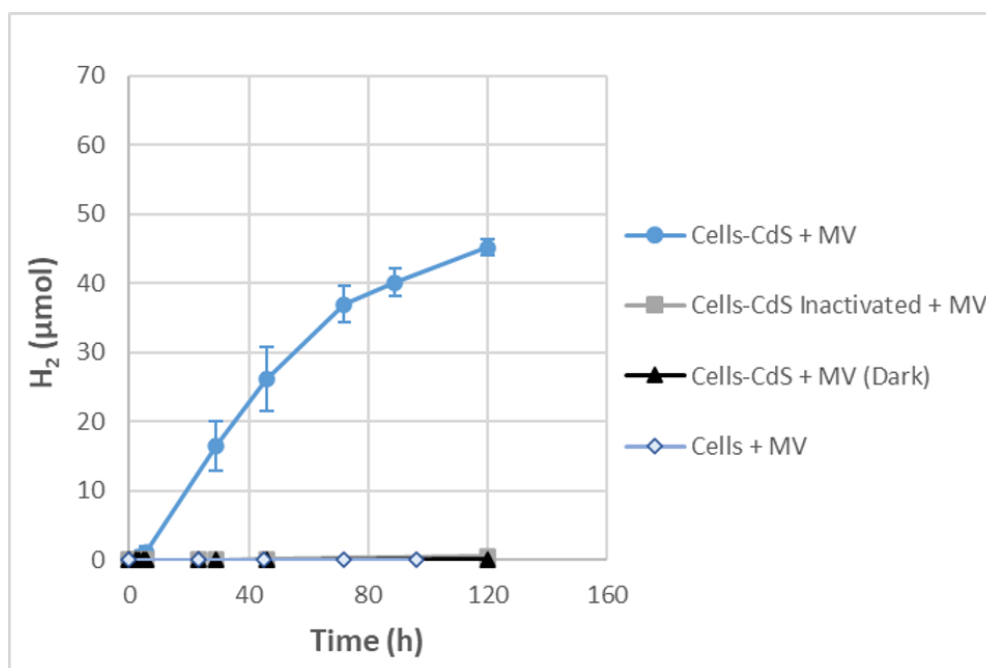
Figure 3.16. - Hydrogen photoproduction profile by *Desulfovibrio desulfuricans*-CdS and its respective controls. Error bars indicate the standard deviations of the average values.

Thus, these experiments demonstrated that *D. desulfuricans* is only able to produce H_2 in the presence of its biological CdS precipitates when the biohybrid is exposed to an energy source, generating a considerable amount of hydrogen in these conditions.

3.1.4.3. - Effect of Cd concentration in H_2 production by Desulfovibrio desulfuricans-CdS system

The influence of Cd concentration on H_2 production by biohybrid system was investigated. The concentrations used to synthesize the *D. desulfuricans* semiconductor were: 0.5, 1, 2, 3 and 4 mM of Cd, in presence of MV (**Figure 3.17.**).

D. desulfuricans-CdS presented the highest H_2 production with 2 and 3 mM of Cd, reaching ~20 μmol of H_2 after 22 h of light exposure (**Figure 3.17.**). In presence of lower Cd concentrations (<1 mM), the cells probably do not generate enough semiconductor for an efficient light-harvesting process. Conversely, Cd concentrations higher than 3 mM decreased the biohybrid activity, possibly due to toxicity (**Figure 3.17.**).
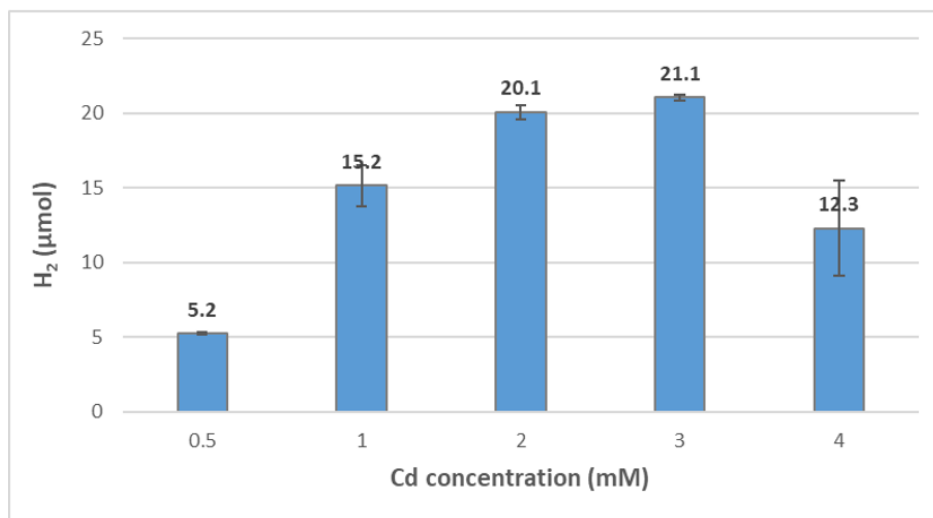

Figure 3.17. - Effect of Cd concentration on H_2 production by *Desulfovibrio desulfuricans*-CdS. Data from 22 h. The error bars indicate standard deviation of the average values.

Therefore, the optimal Cd concentrations for *D. desulfuricans*-CdS system were 2 and 3 mM. Hence, further experiments using biocatalyst *Desulfovibrio desulfuricans* were all performed with 3 mM of Cd.

3.1.4.4. - Effect of electron shuttle in H_2 production by Desulfovibrio desulfuricans-CdS system

To investigate the impact of electron mediator in H_2 production by *Desulfovibrio desulfuricans*-CdS, photocatalytic experiments were performed in presence and absence of MV (**Figure 3.18.**).

D. desulfuricans-CdS/MV produced a considerable amount of H_2 (56.1±5.1 µmol) after 142 h, with a specific H_2 production rate of 418.3 µmol g_{dcw}^{-1} h^{-1} (**Figure 3.18.**). The H_2 production of biohybrid started to stabilize after 45 h of light exposure (at 46.0±4.8 µmol of H_2), that could be related to depletion of sacrificial electron donor. In absence of MV, the system had also a significant H_2 production with 31.7±8.1 µmol, but it did not reach a plateau (**Figure 3.18.**). The specific H_2 production rate of *D. desulfuricans*-CdS without electron shuttle was 48.9 µmol g_{dcw}^{-1} h^{-1}.
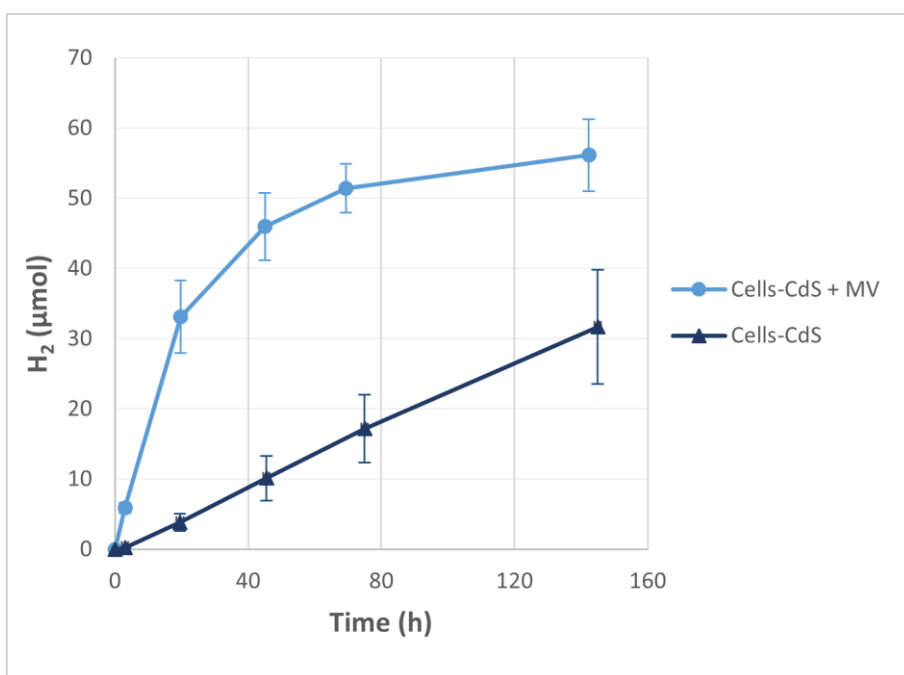

Figure 3.18. - Effect of MV in H_2 production by *Desulfovibrio desulfuricans*-CdS system. The error bars indicate the standard deviations of the average values.

Thus, *D. desulfuricans*-CdS generated a substantial H_2 amount in presence of MV. However, the system also produced H_2 without the assistance of an

electron mediator, proving that cells can accept electrons directly from CdS semiconductor.

3.1.5. - Biohybrid Escherichia coli-CdS system

3.1.5.1. - Creation of Escherichia coli-CdS system

Since *Escherichia coli* was the only biocatalyst investigated for H_2 production through self-photosensitization with NPs strategy (**Figure 1.4.**)[50–52], we constructed a *E. coli*-CdS biohybrid as a control system and compared with the new photocatalytic systems developed.

Thus, *Escherichia coli* was also able to synthesize CdS semiconductor in presence of 1 mM of Cd, as illustrated by the color difference of medium (that turned to a yellowish CdS color after the addition of Cd) (**Figure 3.19.**).
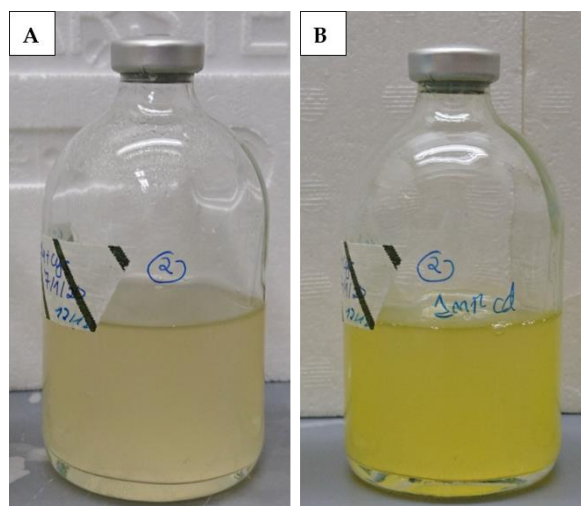
Figure 3.19. - Difference of color in medium inoculated with *Escherichia coli*, in absence of Cd (**A**) and with 3 h of incubation with 1 mM of Cd (**B**).

SEM images showed that nanoparticles are only formed on the surface of *E. coli* cells when cadmium is added to bacteria, (**Figure 3.20.**). The CdS NPs are distributed between all cells with different intensities (some bacteria precipitates are more concentrated than others) (**Figure 3.20 B.**). Hence, these results demonstrated the effective creation of *E. coli*-CdS system.
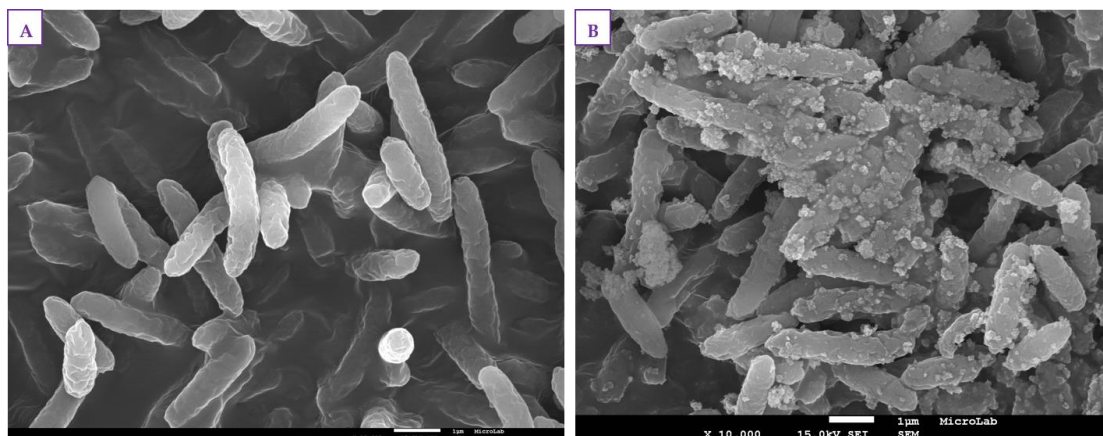
Figure 3.20.- Characterization of *Escherichia coli*-CdS. SEM images of *Escherichia coli* (**A**) and *Escherichia coli*-CdS biohybrid (**B**).

3.1.5.2. - H_2 production profile of Escherichia coli-CdS system

To assess H_2 production performance of *Escherichia coli*-CdS system, a series of photocatalytic assays were conducted to determine the optimal conditions to achieve higher H_2 production.

E. coli-CdS/MV system produced 9.1±1.8 µmol of H_2 after 137 h of light exposure, with a specific H_2 production rate of 9.3 µmol g_{dcw}^{-1} h^{-1} (**Figure 3.21.**).

Relative to control experiments, performed in presence of MV, both *E. coli*-CdS under dark conditions and grown *E. coli* without the self-produced semiconductor, did not produce H_2. Conversely, inactivated *E. coli*-CdS system had a residual H_2 production of 1.2±1.8 µmol after 145 h (**Figure 3.21.**), like inactivated *C. freundii*-CdS and *D. desulfuricans*-CdS systems.
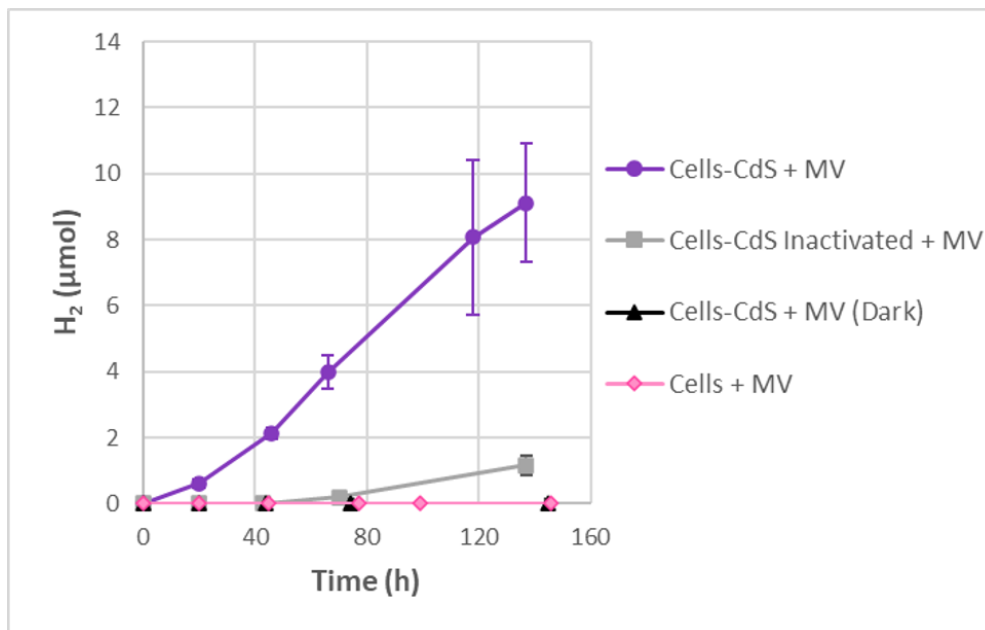
**Figure 3.21. -** Hydrogen photoproduction profile by *Escherichia coli-CdS* and its respective controls. Error bars indicate the standard deviations of the average values.

Therefore, these experiments confirmed that H_2 production is only possible when *Escherichia coli* is associated with CdS semiconductor, when system was exposed to a light source.

3.1.5.3. - Effect of Cd concentration in H_2 production by Escherichia coli-CdS system

To study the effect of cadmium concentration on biohybrid H_2 production, different Cd concentrations were tested to synthetize *E. coli* semiconductor (**Figure 3.22.**).

E. coli-CdS systems constructed with 0.5 and 1 mM of Cd achieved highest H_2 production with ~3.5 μmol, after 47 h under LED lights. On the contrary, higher Cd concentrations (>1 mM) resulted in lower H_2 production (**Figure 3.22.**).
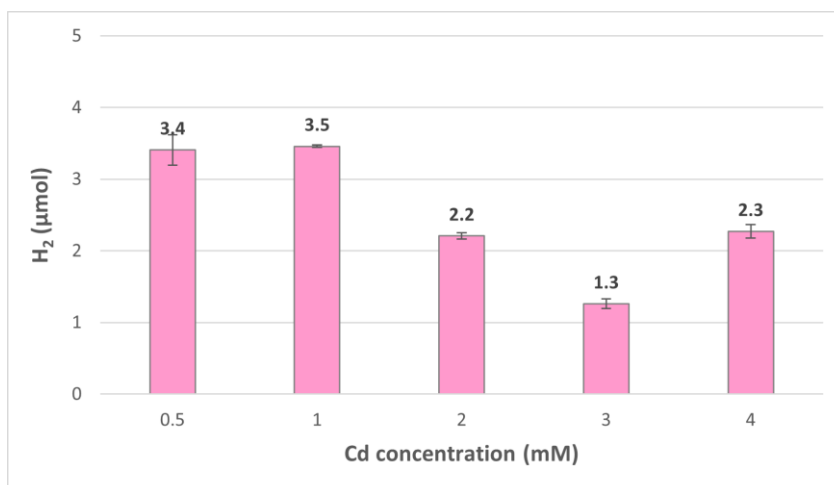
Figure 3.22. - Effect of Cd concentration on H_2 production by *Escherichia coli*-CdS. Data is from 47h. The error bars indicate standard deviation of the average values.

The increased of Cd concentration also led to lower H_2 production performances of *C. freundii* and *D. desulfuricans* biohybrids systems, but only for concentrations higher than 4 mM (**Figure 3.6.**, **Figure 3.17.**). In the case of *E. coli*-CdS system developed by Wang *et. al*[50], they also tested different Cd concentrations to induce NPs precipitation on *E. coli* cell surface. The optimal Cd concentration found for that system was 0.3 nM, where higher concentrations resulted in the decrease of cell density[50]. Additionally, it has been reported that CdS nanoparticles induce several stress responses systems and morphology changes in *E. coli* cells[124,125].

Hence, higher Cd concentrations seems to be toxic to *E. coli* cells. Thus, lower concentrations appear to be more appropriate to construct the biophotocatalytic system using *E. coli* as biocatalyst.

3.1.5.4. - Effect of electron shuttle in H_2 production by Escherichia coli-CdS system

The impact of electron shuttle in H_2 production by *E. coli*-CdS was studied. Thus, photocatalytic assays were performed with *E. coli*-CdS system with the optimal Cd concentration (1 mM of Cd) in presence and absence of MV (**Figure 3.23.**).

E. coli-CdS/MV system had a hydrogen production of 9.1±1.8 µmol, whereas in absence of electron mediator biohybrid only produced 3.0±0.5 µmol of H_2, after 137 h of light exposure (**Figure 3.23.**). The specific H_2 production rate with and without MV was 9.3 and 2.9 µmol g_{dcw}^{-1} h^{-1}, respectively.
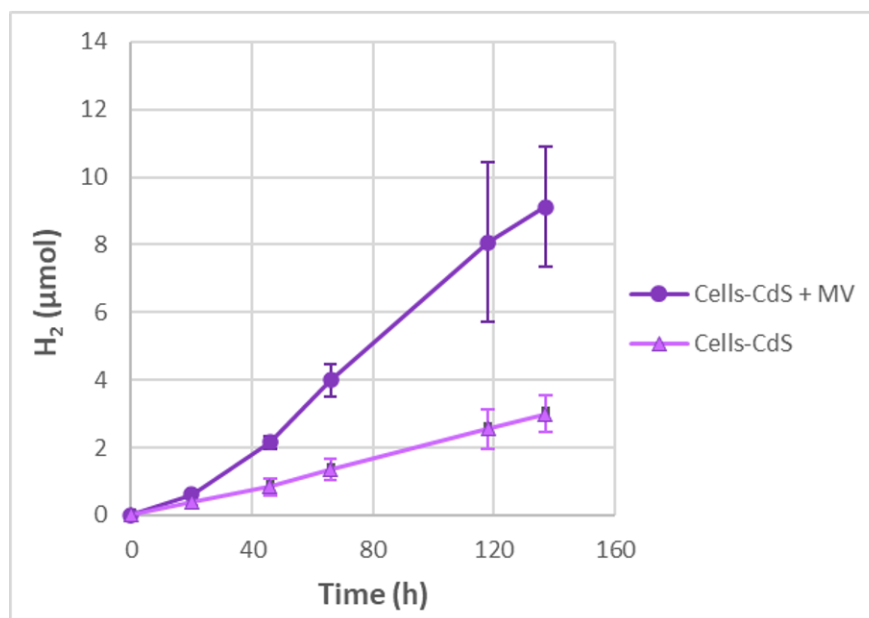
Figure 3.23. - Effect of MV in H_2 production by *Escherichia coli*-CdS system. The error bars indicate the standard deviations of the average values.

Biohybrid systems developed by Wang *et al.*, namely using *E. coli* and self-produced CdS and Ag/In_2S_3, a main electron donor (glucose) was required for H_2 production[50,51]. Moreover, in engineering *E. coli* surface-display system, created by Wei and coworkers, MV was needed for H_2 photoproduction[52]. In this study, *E. coli*-CdS system presented only a modest activity for light-driven H_2 production in the absence of glucose (**Figure 3.23.**).

3.1.6. - Comparison between the proposed biocatalysts-CdS systems for H$_2$ photoproduction

To sum up, from the potential four biocatalysts tested and the *E. coli* control system, three of them were able to both generate CdS nanoparticles and produce H$_2$: *C. freundii*-CdS, *D. vulgaris*-CdS, *D. desulfuricans*-CdS and *E. coli*-CdS biohybrid systems (**Table 3.1.**).

The most efficient photocatalytic system was the one where *D. desulfuricans* was used as biocatalysts, where H$_2$ production was superior both in the presence and absence of MV, when compared with the other systems (**Table 3.1.**). Relative to *C. freundii*-CdS, *D. vulgaris*-CdS and *E. coli*-CdS biohybrids, they produced H$_2$ in the same magnitude. *C. freundii*-CdS and *E. coli*-CdS systems reached a higher H$_2$ production in the presence of MV, whereas *D. vulgaris*-CdS generated higher H$_2$ amounts without MV (**Table 3.1.**).

Table 3.1.- Hydrogen production and H$_2$ production rates of biohybrid systems (from light) and whole-cells (from dithionite-reduced MV).

Biocatalyst	Biohybrid systems + light (μmol g$_{dcw}^{-1}$)		Biohybrid systems + light (μmol g$_{dcw}^{-1}$ h^{-1})		Whole-cells (μmol g$_{dcw}^{-1}$ min^{-1})
	+MV	-MV	+MV	-MV	+MV$_{red}$
C. freundii	827±193	327±75	7.8±0.5	1.8±0.0	1.6±0.1
D. vulgaris	315±121	1289±162	2.1±0.2	9.2±0.1	293±7
D. desulfuricans	12384±1130	6984±1798	418±26	49±1	280±9
E. coli	1199±234	394±72	9.3±0.5	2.9±0.1	3.7±0.1

The high efficiency of *D. desulfuricans*-CdS system is probably related with the high hydrogenase activity present in this organism. Thus, hydrogenase activity of the four organisms was determined using MV reduced with excess of dithionite as electron donor (**Table 3.1.**), (**Figure A2.**).

D. desulfuricans cells showed a high hydrogenase activity followed by *E. coli* and *C. freundii* with the values 280, 3.7 and 1.6 μmol g$_{dcw}^{-1}$ min^{-1}, respectively,

which agrees with the relative values of the photosynthetic H_2 production rates obtained with biohybrid systems from light (**Table 3.1.**) (**Figure A2 A-C.**). *D. desulfuricans* is characterized by a high level of hydrogenases[54], most of which are present in the periplasm and are thus likely to be more efficient in receiving electrons directly from CdS nanoparticles than intracellular hydrogenases.

Moreover, *D. vulgaris* presented a high hydrogenase activity of 293 µmol $g_{dcw}^{-1}min^{-1}$ (**Table 3.1.**) (**Figure A2 D.**). This finding is in accordance with the high number of hydrogenases and the great catalytic rate of [NiFeSe] enzyme of *D. vulgaris*[54,60,61]. The two SRB microorganisms studied *D. desulfuricans* and *D. vulgaris* have a very similar hydrogenases activity (**Table 3.1.**). However, as mentioned before, *D. desulfuricans*-CdS biohybrid had the highest H_2 production between all biohybrid systems, which strongly suggests that the much lower H_2 production obtained with *D. vulgaris*-CdS biohybrid is related with electron transfer process from CdS semiconductor to cells.

Therefore, the best and most suitable biocatalyst for light-driven H_2 production between the proposed four biocatalysts is *Desulfovibrio desulfuricans*. Hence, the following studies were only performed using *D. desulfuricans*-CdS biohybrid system with 3 mM of Cd.

3.1.7. - Effect of sacrificial electron donor in H_2 photoproduction

Since *D. desulfuricans* was the selected biocatalyst to construct the biohybrid and also the only system that achieved a plateau after 45 h of light irradiation (**Figure 3.18.**), the effect of sacrificial electron donor, HCl-cysteine, in H_2 production was tested. Hydrogen photoproduction by *D. desulfuricans*-CdS was evaluated under different amounts of HCl-cysteine: 0, 59, 99 and 182 µmol. The experiments were carried out in presence of MV (**Figure 3.24.**).

Without the cysteine, biohybrid only produced 5.1 µmol of H_2 (**Figure 3.24.**), showing that biohybrid system requires the sacrificial electron donor to operate. The assays performed with 59, 99 and 182 µmol produced 34.6±1.2, 50.1±4.2 and 79.9±8.1 µmol of H_2, respectively, after 44 h of light irradiation (**Figure 3.24.**) and

then H_2 production stabilized. SED allows the continuous cycle of electron transfer from CdS nanoparticles to hydrogenases by quenching the electron *holes* from semiconductor; without this *hole* scavengers the cycle is interrupted and hydrogen production ceases.

It was observed that H_2 production increased with the increase in cysteine amount (**Figure 3.24.**), indicating that SED also accelerates the generation of H_2. The increase of H_2 production with the increase of cysteine has been reported in other studies[47,126]. The hydrogen yields for 59, 99 and 182 µmol of cysteine were 117%, 101% and 88%, respectively (**Equation 2.1.**, **Equation 2.2.**). A slight amount of H_2 (5.1 µmol) was produced without the addition of the sacrificial electron donor, which explains the H_2 yield superior to 100%.

Hence, these results demonstrated that the biohybrid system requires a sacrificial electron donor to function, confirming that the cessation of H_2 production observed under LED illumination is caused by cysteine depletion.
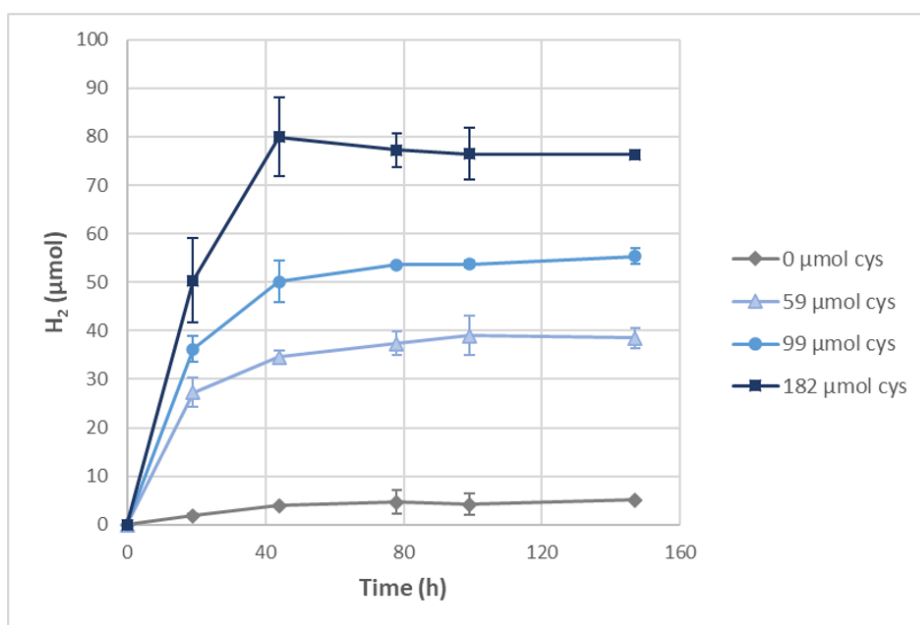
Figure 3.24. - Effect of SED in H_2 production by *Desulfovibrio desulfuricans*-CdS system. The error bars indicate the standard deviations of the average values.

3.2. – Selection of best semiconductor combination for biohybrid H$_2$ photoproduction

Although CdS nanoparticles are an excellent semiconductor for light-driven H$_2$ production, they also present low photo-stability and high recombination rate of photo-induced electron-*hole* pairs, when exposed to visible light for a long time[79,80]. Hence, three earth-abundant metals (tungsten, nickel and molybdenum) were used as cocatalysts in *Desulfovibrio desulfuricans*-CdS biohybrid system, to improve H$_2$ production. To our knowledge, this is the first time that cocatalysts were used in a self-photosensitization photocatalyst system.

Thus, the construction of *D. desulfuricans*-CdS-WS$_2$, *D. desulfuricans*-CdS-NiS and *D. desulfuricans*-CdS-MoS$_2$ were performed and the impact of cocatalysts in H$_2$ production was studied. Since *D. desulfuricans*-CdS without MV generated a significant amount of H$_2$ (31.7±8.1 μmol) (**Figure 3.18.**), the studies from now on were only performed with the biocatalyst without the electron shuttle. The photocatalytic assays were performed under LEDs light (with 0.042 mW cm^{-2} of irradiance).

3.2.1.- Effect of cocatalyst concentration in H$_2$ photoproduction by Desulfovibrio desulfuricans-CdS system

To assess the effect of cocatalysts in H$_2$ production, different concentrations of W, Ni and Mo were used to construct the binary CdS-based semiconductor of *D. desulfuricans*-CdS biohybrid (**Figure 3.25.**). Hydrogen production by the systems loaded with cocatalysts were compared with *D. desulfuricans* with 3 mM of Cd (control experiment). Hydrogen content was measured after 44 h of light exposure (**Figure 3.25.**):
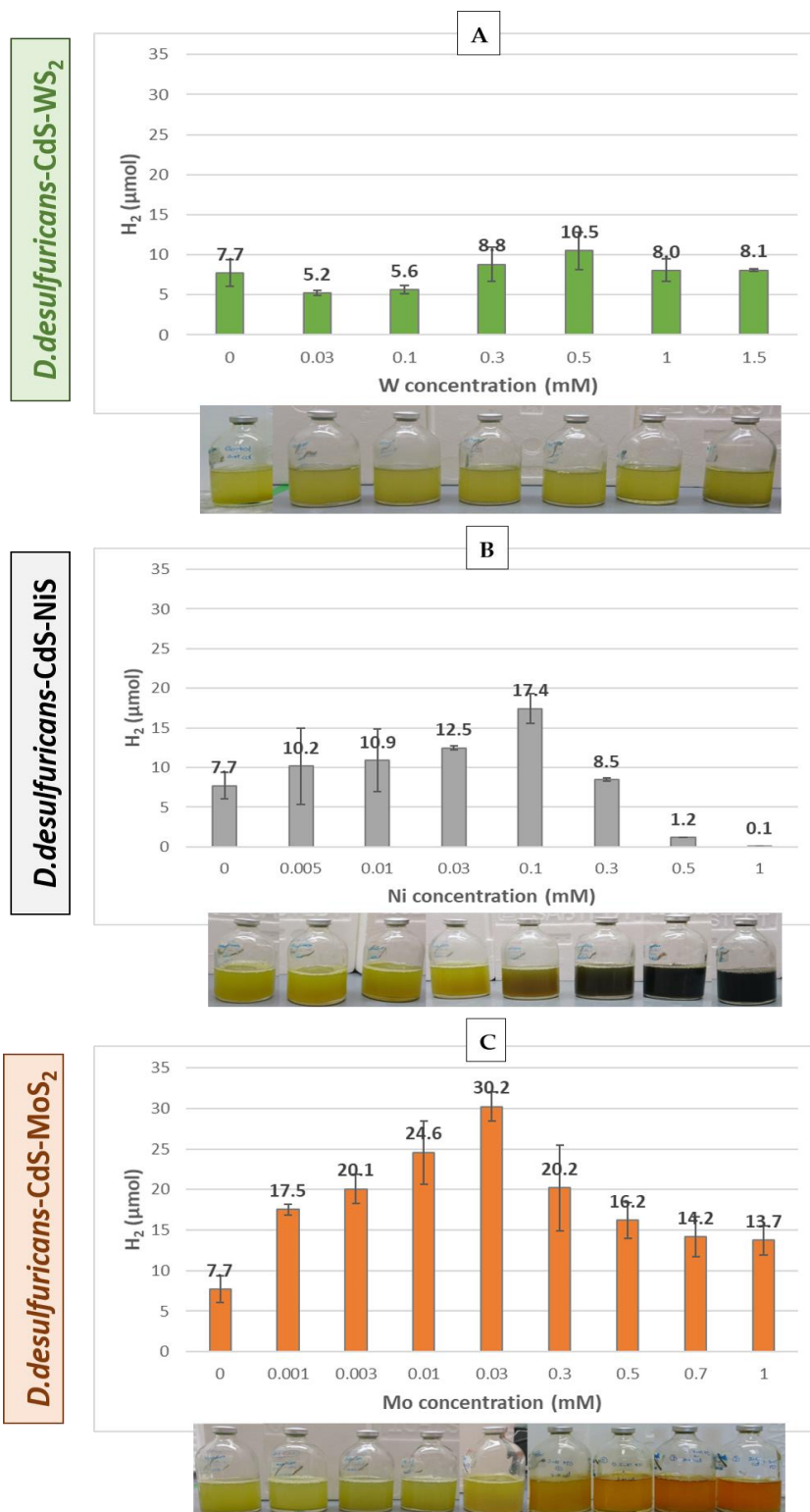
Figure 3.25. - Effect of cocatalyst concentration in H_2 production by *Desulfovibrio desulfuricans*-CdS, for 44 h. H_2 production profile by biohybrid system with different concentrations of tungstate (**A**), nickel (**B**) and molybdenum (**C**) and its respective impact in medium color (after cocatalyst addition). Error bars indicate the standard deviations of the average values.

The addition of tungsten did not change medium color, thus presenting the characteristic yellow color of CdS (**Figure 3.25 A.**). Moreover, the maximum of H_2 generated with *D. desulfuricans*-CdS loaded with tungsten was 10.5±2.4 µmol (using 0.5 mM of W), which was in the same magnitude of H_2 generated by the control experiment (7.7±1.7 µmol) (**Figure 3.25 A.**). Therefore, the addition of tungsten did not have a great impact in H_2 production of biohybrid system.

As illustrated in **Figure 3.25 B.**, the addition of nickel to *D. desulfuricans*-CdS provoked a change of color in the medium. The media turned progressively darker with the increase of cocatalyst concentration, acquiring a black color (characteristic of nickel sulfide[127]), at higher Ni concentrations (>0.1 mM) (**Figure 3.25 B.**). The maximum H_2 production was achieved with *D. desulfuricans*-CdS composed with 0.1 mM of Ni, generating 17.4±1.9 µmol of H_2 (**Figure 3.25 B.**), that was higher than H_2 production by system without cocatalyst (7.7±1.7 µmol). Additionally, systems loaded with lower Ni concentrations (<0.1 mM) and 0.3 mM, were able to produce H_2, conversely to higher Ni concentrations where residual H_2 were generated (**Figure 3.25 B.**). Therefore, these results indicate that Ni can enhance H_2 production (in presence of lower cocatalyst concentrations), suggesting that higher amounts of Ni could be toxic to cells or that the acquired black color of medium hinders the access of light by biohybrid.

D. desulfuricans-CdS-MoS$_2$ biohybrids were constructed with a wide range of Mo concentrations: from 0.001 to 1 mM (**Figure 3.25 C.**). The medium inoculated with *D. desulfuricans* and Cd suffer a color change in presence of higher concentrations of Mo (>0.03 mM), developing a gradually intense orange color with the increase of cocatalyst concentration (**Figure 3.25 C.**). Notably, molybdenum disulfide (MoS$_2$) presents a brown color[128], thereby the obtained orange color is possibly the result of the yellowish color acquired from CdS conjugated with the brown of MoS$_2$. All biohybrid systems loaded with Mo, registered a superior H_2 production than *D. desulfuricans*-CdS (7.7±1.7 µmol), regardless of Mo concentration used. *D. desulfuricans*-CdS with 0.03 mM of Mo presented the highest and an impressive H_2 production of 30.2±1.8 µmol, that was almost 4 times higher than the H_2 generated by the control experiment

(**Figure 3.25 C.**). Thus, it has been demonstrated that molybdenum is an excellent cocatalyst for the proposed photocatalytic system to enhance H_2 production.

In summary, the addition of the cocatalysts improved H_2 photoproduction of *Desulfovibrio desulfuricans*-CdS system, but with different magnitudes (**Figure 3.25.**). From the three cocatalysts tested, molybdenum had the greatest impact on biohybrid H_2 production, followed by nickel and tungsten.

3.2.2.- Characterization of Desulfovibrio desulfuricans-CdS loaded with cocatalysts

Since the effectiveness of loading cocatalysts in the biohybrids was proven (**Figure 3.25.**), the systems *D. desulfuricans*-CdS-WS$_2$, *D. desulfuricans*-CdS-NiS and *D. desulfuricans*-CdS-MoS$_2$ were characterized by SEM (**Figure 3.26.**).

In *D. desulfuricans* with 3 mM of Cd (the control system), CdS precipitated on cells surface with great intensity, covering all *D. desulfuricans* bacteria (**Figure 3.26 A.**). Conversely, biohybrid with 1 mM of Cd presented less CdS precipitates, which were concentrated in just a couple of cells (**Figure 3.15 B.**). Thus, the increase of Cd concentration (from 1 to 3 mM) allowed not only the increase of CdS precipitates, but also its even distribution among *D. desulfuricans* cells. These findings could be the reason why photocatalytic system with 3 mM of Cd is more efficient than biohybrid constructed with 1 mM of Cd (**Figure 3.16.**, **Figure 3.18.**).

Moreover, SEM images of biohybrid systems loaded with tungsten (**Figure 3.26 B.**), nickel (**Figure 3.26 C.**) and molybdenum (**Figure 3.26 D.**), shows CdS precipitates on cell surface with high intensity, similarly to the control system (**Figure 3.26 A.**). Therefore, it was hypothesized that cocatalysts aggregates/forms a complex with cadmium sulfide nanoparticles, originating precipitates of CdS-NiS (**Figure 3.26 B.**), CdS-WS$_2$ (**Figure 3.26 C.**) and CdS-MoS$_2$ (**Figure 3.26 D.**) on *Desulfovibrio desulfuricans* surface.

D.desulfuricans-CdS

D.desulfuricans-CdS-WS$_2$

D.desulfuricans-CdS-NiS

D.desulfuricans-CdS-MoS$_2$
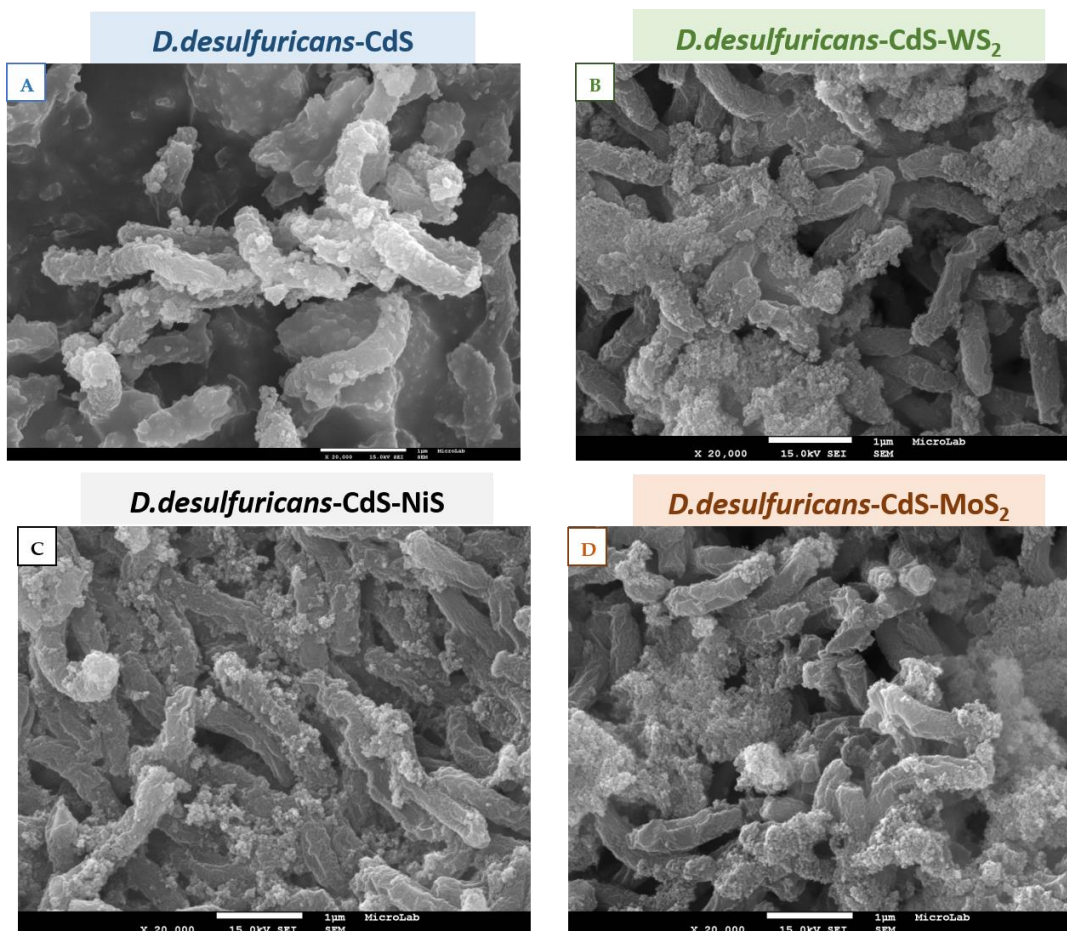
Figure 3.26. - Characterization of *Desulfovibrio desulfuricans*-CdS with cocatalysts. SEM images of Desulfovibrio desulfuric*ans*-CdS (**A**), *D. desulfuricans*-CdS-WS$_2$ (**B**), *D. desulfuricans*-CdS-NiS (**C**) and *D. desulfuricans*-CdS-MoS$_2$ (**D**) biohybrids.

3.2.3.- H$_2$ production profile of Desulfovibrio desulfuricans-CdS loaded with optimal cocatalysts concentrations

A H$_2$ production profile for *D. desulfuricans*-CdS-WS$_2$, *D. desulfuricans*-CdS-NiS and *D. desulfuricans*-CdS-MoS$_2$ systems was obtained and compared with *D. desulfuricans*-CdS (control system) (**Figure 3.27.**). The biohybrids were constructed using 3 mM of Cd conjugated with the optimal cocatalyst concentration previously determined, particularly 0.5, 0.1 and 0.03 mM for W, Ni and Mo, respectively (**Figure 3.25.**).

D. desulfuricans-CdS with 0.03 mM of Mo had the highest H_2 production with 49.7±1.3 µmol of H_2 after 147 h of irradiation with a specific H_2 production rate of 130.8 µmol $g_{dcw}^{-1}h^{-1}$ (**Figure 3.27., Table 3.2.**). Moreover, biohybrid loaded with 0.1 mM of Ni generated 40.6±0.6 µmol of H_2 (whit a specific H_2 production rate of 87.2 µmol $g_{dcw}^{-1}h^{-1}$), whereas *D. desulfuricans*-CdS with 0.5 mM W produced 32.1±2.5 µmol of H_2 at a specific rate of 57.4 µmol $g_{dcw}^{-1}h^{-1}$. *D. desulfuricans*-CdS, in turn, had a H_2 production of 21.9±3.4 µmol with a specific H_2 production rate of 34.0 µmol $g_{dcw}^{-1}h^{-1}$ (**Figure 3.27., Table 3.2.**).

Hence, the systems loaded with cocatalysts all presented superior H_2 performances than *D. desulfuricans*-CdS, the control system (**Figure 3.27.**). The addition of cocatalysts not only allowed the generation of higher amounts of H_2, but also enhanced the rate of its production, thereby systems with cocatalysts achieved higher H_2 content in a shorter period time (**Table 3.2.**).
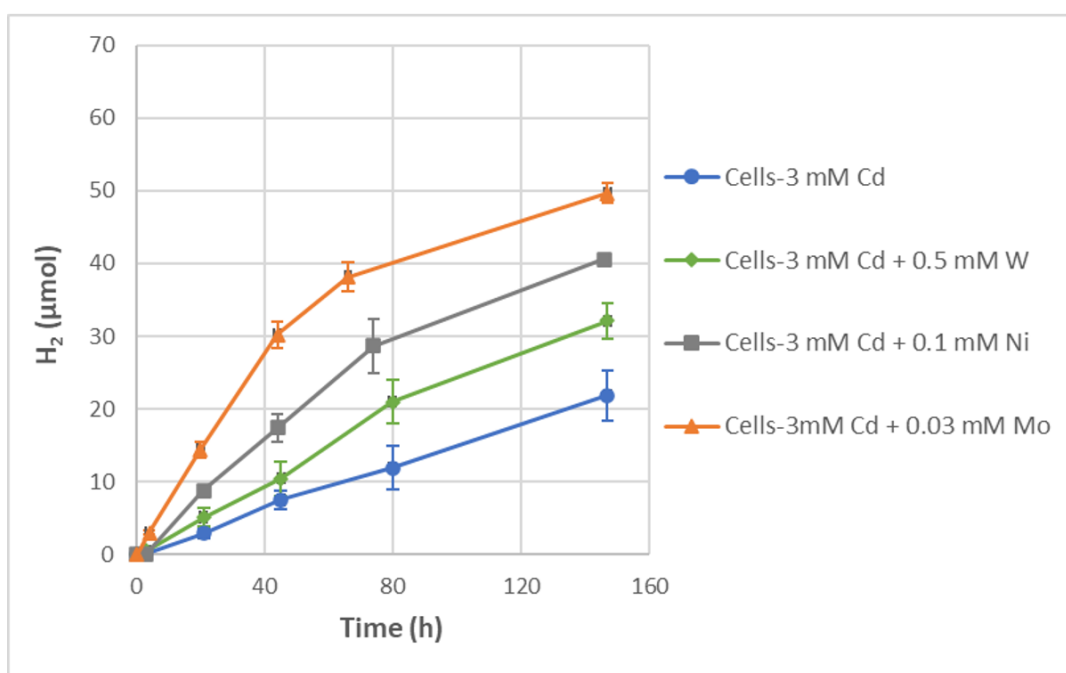
Figure 3.27. - Hydrogen photoproduction profile of *D. desulfuricans*-CdS (3 mM of Cd) loaded with cocatalyst (W, Ni or Mo). The cocatalysts concentrations were 0.5 mM for W, 0.1 mM for Ni and 0.03 mM for Mo. The error bars indicate the standard deviations of the average values.

Table 3.2.- Effect of cocatalysts (W, Ni and Mo) in H_2 production by *Desulfovibrio desulfuricans*-CdS after 147 h of light irradiation.

Conditions	H_2 (µmol)	Specific H_2 production rate (µmol g_{dcw}^{-1} h^{-1})
Cells-CdS	21.9±3.4	34.0±0.8
Cells-CdS-WS$_2$	32.1±2.5	57.4±2.1
Cells-CdS-NiS	40.6±0.6	87.2±2.6
Cells-CdS-MoS$_2$	49.7±1.3	130.8±9.3

Since *D. desulfuricans*-CdS loaded with 0.03 mM of Mo presented the highest H_2 production, further studies were all conducted with this biohybrid system.

3.3. – Effect of light source on biohybrid system H_2 performance

To investigate the impact of light source on H_2 production by biohybrid system, *D. desulfuricans*-CdS and *D. desulfuricans*-CdS-MoS$_2$ were exposed to different illumination sources (**Figure 3.28**.). The energy sources tested were two violet LEDs that emitted visible light at the same wavelength (λ=445 nm) with irradiances (I) of 0.042 and 3.6 mW cm^{-2} and a solar simulator (Xenon lamp). The violet LED with an irradiance of 0.042 mW cm^{-2} have been the standard light source used in the previous photocatalytic assays.

D. desulfuricans-CdS was able to double its H_2 production from 21.9±3.4 to 43.9±3.6 µmol in 147 h, by exposing the system to a LED light of higher intensity (I=0.042 and 3.6 mW cm^{-2}, respectively) (**Figure 3.28 A.**). The specific H_2 production rate of systems exposed to LEDs of 0.042 and 3.6 mW cm^{-2} were 34.0 and 70.5 µmol $g_{dcw}^{-1}h^{-1}$, correspondingly (**Table 3.3.**). Thus, the increase of LED's

light intensity allowed the increase of H_2 production of *D. desulfuricans*-CdS system by increasing its rate of H_2 production.

Moreover, *D. desulfuricans*-CdS-MoS_2 under LED of higher intensity (I=3.6 mW cm^{-2}) generated 57.1±6.1 µmol of H_2 in only 43 h, reaching a plateau due to cysteine depletion. Conversely, the H_2 production by biohybrid system exposed to LED of I=0.042 mW cm^{-2} never stabilized, producing 49.7±1.3 µmol of H_2 for 147 h (**Figure 3.28 A.**). On the other hand, *D. desulfuricans*-CdS-MoS_2 under solar simulator light reached a H_2 maximum production of 61.9±8.6 µmol in only 4 h and stabilized (**Figure 3.28 B.**). The specific H_2 production rate of systems under LED of I=3.6 and 0.042 mW cm^{-2} were 513.6 and 130.8 µmol $g_{dcw}^{-1}h^{-1}$, respectively, whereas for biohybrid exposed to Xenon lamp light was 3223.0 µmol $g_{dcw}^{-1}h^{-1}$ (**Table 3.3.**).
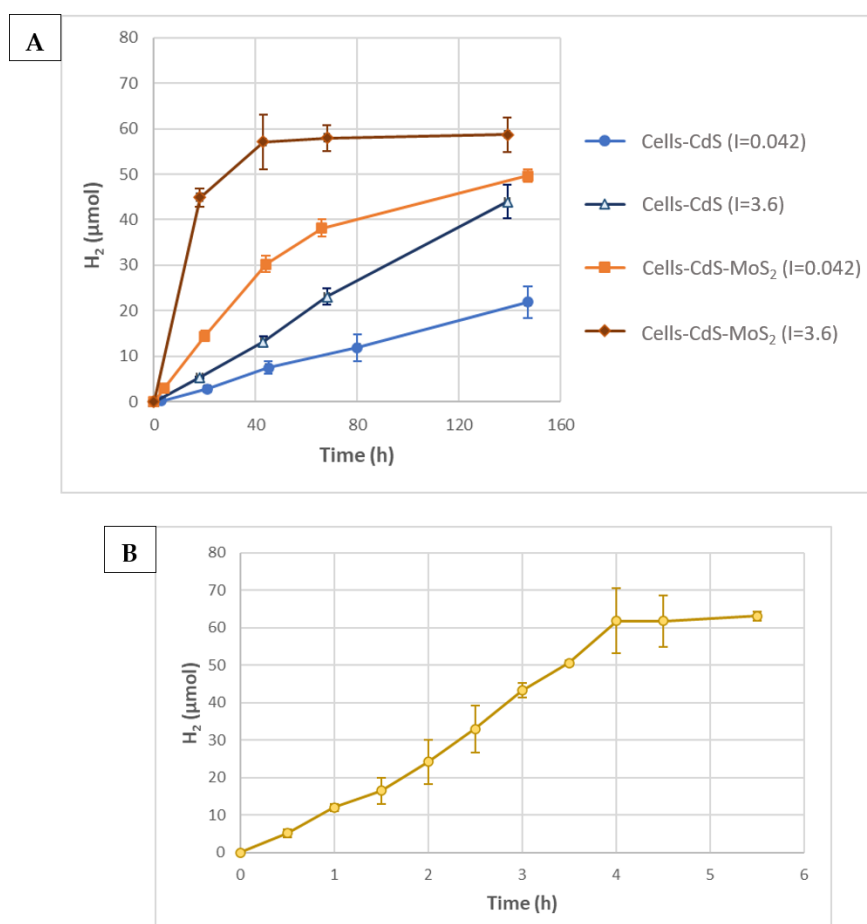
Figure 3.28.- Effect of light source in H_2 photoproduction by *Desulfovibrio desulfuricans*-CdS-MoS_2 under LEDs (with irradiances of 3.6 and 0.042 mW cm^{-2}) (A) and solar simulator (B). The Error bars indicates the standard deviations of average values.

Table 3.3.- Effect of light sources (LEDs and solar simulator) in H_2 production by *Desulfovibrio desulfuricans*-CdS-MoS$_2$.

Conditions	H$_2$ (µmol)	Specific H$_2$ production rate (µmol g$_{dcw}^{-1}$ h^{-1})
Cells-CdS (I=0.042)	21.9±3.4	34.0±0.8
Cells-CdS (I=3.6)	43.9±3.6	70.5±1.9
Cells-CdS-MoS$_2$ (I=0.042)	49.7±1.3	130.8±9.3
Cells-CdS-MoS$_2$ (I=3.6)	57.1±6.1	513.6±11.5
Cells-CdS-MoS$_2$ (solar simulator)	61.9±8.6	3223.0±117.0

Hence, the increase of light source intensity (namely with LED of I=3.6 mW cm^{-2} and solar simulator) enables the increase of H$_2$ production rate (since more energy was supplied to the system), allowing the biohybrid to achieve its maximum H$_2$ production (limited by SED depletion) quicker. Similarly, other biophotocatalytic systems also verified an enhancement of H$_2$ production with the increase of light intensity[19,50]. Therefore, the energy source provided for photocatalytic assays has a great impact on H$_2$ photoproduction by biohybrid systems.

The apparent quantum yield (AQY) of *D. desulfuricans*-CdS and *D. desulfuricans*-CdS-MoS$_2$ systems under LEDs illumination (with λ=445 nm and irradiance of 0.042 and 3.6 mW cm^{-2}) was determined, assuming that all emitted light was harvested by the system which underestimates the AQY (**Equation 2.3.**). The AQY of *D. desulfuricans*-CdS system was calculated using the first 147 and 139 h, under LED lights of 0.042 and 3.6 W cm^{-2} and with 99 µmol of cysteine. Under these conditions the biohybrid was able to produce 21.9 and 43.9 µmol of H$_2$ with LED of irradiance of 0.042 and 3.6 W cm^{-2}, correspondingly. The AQY of *D. desulfuricans*-CdS-MoS$_2$ was calculated using the first 147 and 43 h, where

system produced 49.7 and 57.1 µmol when exposed to LED of 0.042 and 3.6 W cm^{-2}, respectively.

D. desulfuricans-CdS exposed to LED of 0.042 and 3.6 mW cm^{-2} of irradiation presented an AQY of 3.2 and 0.1 %, correspondingly (**Table 3.4.**). Moreover, an AQY of 7.3 and 0.3 % was achieved with *D. desulfuricans*-CdS-MoS$_2$ under LED of 0.042 and 3.6 mW cm^{-2}, respectively (**Table 3.4.**). The AQY of *D. desulfuricans*-CdS-MoS$_2$ exposed to LED of 0.042 mW cm^{-2} was higher than most biohybrid systems with self-produced semiconductor nanoparticles[39,47,50,51,126] and superior to AQY of plants or algae (0.2-1.6 %[129]).

Table 3.4.- AQY of *Desulfovibrio desulfuricans*-CdS and *Desulfovibrio desulfuricans*-CdS-MoS$_2$ under LEDs lights (I=0.042 and 3.6 mW cm^{-2}).

Biohybrid system	LED irradiance (mW cm^{-2})	AQY (%)
D. desulfuricans-CdS	I= 0.042	3.2
	I= 3.6	0.1
D. desulfuricans-CdS-MoS$_2$	I= 0.042	7.3
	I= 3.6	0.3

3.4. – Immobilization of biohybrid system

The major bottleneck in biohydrogen (BioH$_2$) production is its low yield and H$_2$ production rate in large-scale processes[130–132]. One of the main causes of ineffective industrial BioH$_2$ production is due to biocatalyst wash-out during continuous processes[130,131]. The use of immobilized cells, instead of suspended cells, can be an attractive approach to address this issue. Cell immobilization techniques present many advantages, including: *1)* the increase of biocatalyst stability, *2)* the extension of microbial activity during continuous processes, *3)* the prevention of wash-out, allowing biocatalyst recovery and reutilization and *4)*

easier product separation, which reduces processing costs, making scale-up bioprocess possible[130–133].

Cell entrapment is the simplest and most frequently used method for biohydrogen-producing microorganisms' immobilization[131,132]. In this technique cells are entrapped inside a rigid support matrix (to prevent cell release into reaction medium), where the material is porous enough to allow the diffusion of substrates and products. Thus, the gel matrix not only creates a protective barrier around the biocatalysts, but also ensure its prolonged use and stability[131,132].

Several materials have been considered for cell immobilization purposes. Gel-forming polymers from natural sources have gained much attention due to their biodegradability, renewability, biocompatibility and non-toxicity properties, specially alginate hydrogels[102,134]. Additionally, calcium alginate beads are easy to prepare, low-cost and provide mild conditions for cell immobilization, thereby presenting a high potential for industrial applications[102,132,134,135].

Therefore, *Desulfovibrio desulfuricans*-CdS-MoS$_2$ was immobilized by an entrapment technique using calcium alginate beads. In **Figure 3.29.**, is illustrated *D. desulfuricans*-CdS-MoS$_2$ biohybrid system in suspension *vs.* immobilized in calcium alginate beads. Calcium alginate beads without biohybrid system is colorless (**Figure 3.29 B.**), that acquires the characteristic yellowish color in presence of *D. desulfuricans*-CdS-MoS$_2$ (**Figure 3.29 C.**).

Figure 3.29.- *Desulfovibrio desulfuricans*-CdS-MoS$_2$ system in suspension (**A**) *vs.* immobilized (**C**) in calcium alginate beads (**B**).

The H_2 production profile of *D. desulfuricans*-CdS-MoS$_2$ system immobilized in calcium alginate beads was performed and compared with the system in suspended cells, under LEDs light of 0.042 mW cm^{-2} of irradiance (**Figure 3.30.**).

D. desulfuricans-CdS-MoS$_2$ system immobilized produced 53.3±1.4 µmol of H_2 in 140 h of irradiation, with a specific H_2 production of 83.0 µmol $g_{dcw}^{-1}h^{-1}$. The biohybrid in cell suspension (control system), in turn, generated 47.4±5.7 µmol of H_2 at a specific H_2 production rate of 123.5 µmol $g_{dcw}^{-1}h^{-1}$ (**Figure 3.30.**). Although both systems generated similar H_2 amounts, the immobilized biohybrid initially presented a lower specific H_2 production rate, but H_2 production continued for longer and did not stabilize, contrary to cell suspension system (**Figure 3.30.**). The initial slower H_2 production rate of entrapped *D. desulfuricans*-CdS-MoS$_2$ may be due to a probably decrease of biohybrid activity during the immobilization process or because of diffusional problems (light are less accessible inside the bead). On the other hand, the activity of the immobilized photocatalytic system seems to be extended (the biocatalyst is possibly more protected and stable) (**Figure 3.30.**).
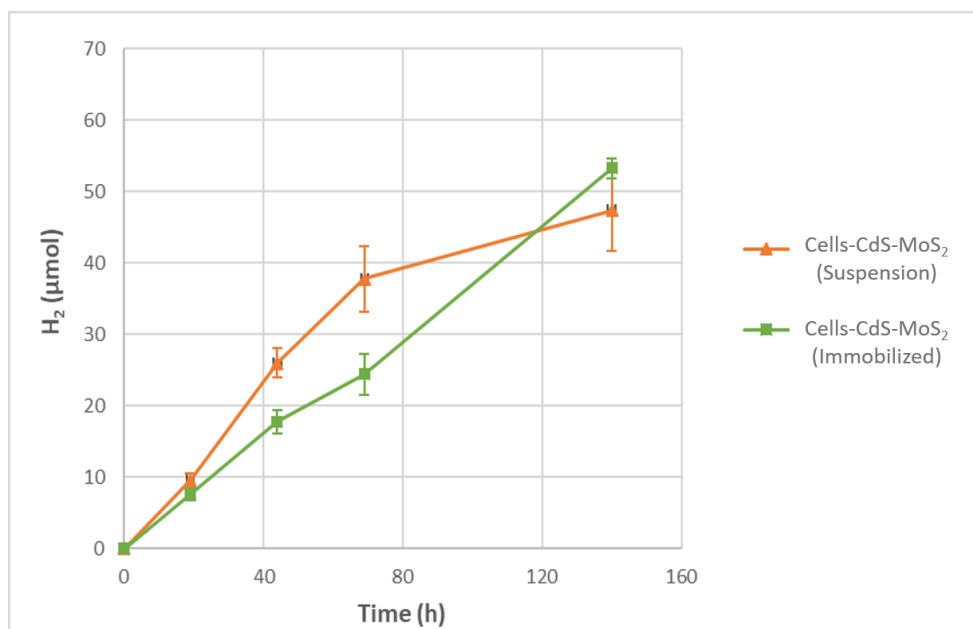
Figure 3.30. - Hydrogen photoproduction profile of *Desulfovibrio desulfuricans*-CdS-MoS$_2$ immobilized in calcium alginate beads *vs.* in suspension. Error bars indicate the standard deviations of the average values.

Hence, not only *D. desulfuricans*-CdS-MoS$_2$ was successfully immobilized in calcium alginate, but it also produced significant H$_2$ amounts. The entrapment of biohybrid system have a great importance in large-scale applications.

3.5. – Development of photocatalytic process for light-driven H$_2$ production

A batch photoreactor for H$_2$ production by *Desulfovibrio desulfuricans*-CdS-MoS$_2$ system was constructed. Moreover, methyl viologen (0.5 mM) was added to the reactor, for a quick detection of H$_2$ production in the photoreactor.

Figure 3.31 A. shows the reactor immediately after the addition of *D. desulfuricans*-CdS-MoS$_2$ (presenting the characteristic yellow color of biohybrid system). In only 1 h 30 min (after photocatalytic system addition), the bioreactor content turned to a blue color, indicating that MV^{2+} is being reduced (**Figure 3.31 B.**).
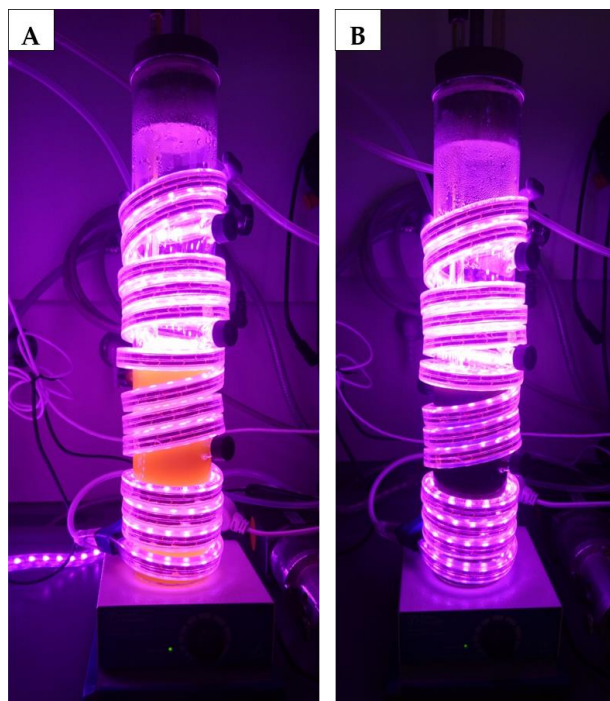
Figure 3.31. - Color evolution in batch reactor at t=0 h (**A**) and t=1h30min (**B**) of functioning.

Hydrogen production by the batch reactor was monitored for 44 h (**Figure 3.32.**). *D. desulfuricans*-CdS-MoS$_2$ produced a significant H$_2$ amount of 4975±152 µmol after 30 h of light exposure, reaching a plateau. The theoretical maximum H$_2$ production was determined, based on **Equation 2.1**. Since the total of cysteine in the reactor was 13.1 mmol, the theoretical maximum H$_2$ determined was 6567 µmol (**Figure 3.32.**). Thus, the efficiency of H$_2$ production by reactor was 76 %. A possible explanation for the biohybrid to not reach the theoretical maximum production could be related to cysteine, that apart from being the sacrificial electron donor of the system is also a reducing agent. Hence, cysteine could have been consumed to reduce some O$_2$ present in the reactor.
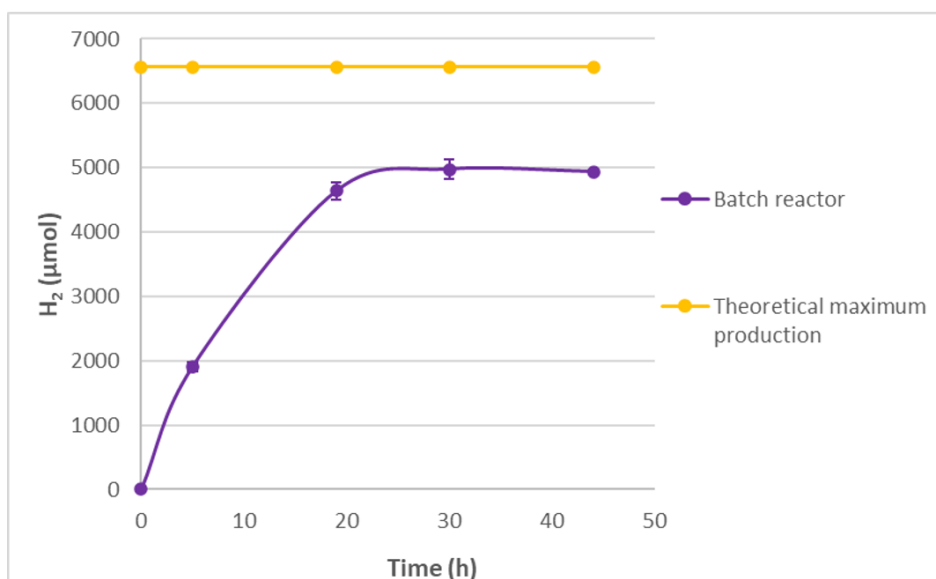
Figure 3.32. - Hydrogen photoproduction of *Desulfovibrio desulfuricans*-CdS-MoS$_2$ system in a batch reactor. Error bars indicate the standard deviation of the average values.

Therefore, a considerable H$_2$ production was attained by *D. desulfuricans*-CdS-MoS$_2$ system in batch bioreactor, in the presence of MV.

4

Chapter 4: Conclusion

The conversion of solar energy to hydrogen is an attractive approach towards a sustainable and low-carbon energy economy. Hence, this thesis aimed to develop a new and more efficient photosynthetic biohybrid system for light-driven H_2 production.

In the present work, among the four systems developed, *D. desulfuricans*-CdS revealed an outstanding H_2 production performance independently of the presence of an electron shuttle. These results demonstrated the ability of *D. desulfuricans* to accept electrons directly from biogenic CdS.

The *D. desulfuricans*-CdS system performance was improved by the addition of cocatalysts, especially with molybdenum, reaching an impressive H_2 production of 49.7 μmol after 147 h of irradiance, which was 2.3 times higher than the system without cocatalyst. The enhancement of H_2 production of biohybrids systems, by employing cocatalysts on the semiconductor, were described and reported for the first time in this thesis.

Moreover, *D. desulfuricans*-CdS-MoS_2 biohybrid was further immobilized in calcium alginate beads. The development of a batch photoreactor for light-driven H_2 production by *D. desulfuricans*-CdS-MoS_2 was also accomplished. In this reactor, the system was able to produce 5 mmol of H_2.

In summary, the construction of a novel and efficient biophotocatalytic system was obtained, showing the importance of exploring novel microorganism and light-harvesting material combinations for production of value-added

products. This work demonstrated the great potential of the biohybrid *D. desulfuricans*-CdS-MoS$_2$ for light-driven H$_2$ production.

5

Chapter 5: Future work

In future work, it would be interesting to investigate the electron transfer from biological CdS to cells of biohybrid systems. Fundamental studies at molecular level, to identify and to better understand the proteins and complexes involved in these processes, would allow to stimulate specific targets for a more efficient electron transfer, for example. Moreover, the strategy for the creation of CdS nanoparticles could be modified for *Clostridium acetobutylicum*, particularly by using other sulfur sources, like hydrogen sulfide.

Additionally, the developed biohybrid system could be explored for other applications, particularly for CO_2-reduction to formate since *D. desulfuricans* also presents formate dehydrogenases.

Moreover, another promising approach to enhance the proposed biophotocatalytic system is the employment of Synthetic Biology tools. These tools would enable the engineering of cell's intracellular metabolism or even the creation of new pathways, to maximize chemicals and fuels production by biohybrid systems.

References

1.   Dawood, F., Anda, M. & Shafiullah, G. M. Hydrogen production for energy: An overview. *Int. J. Hydrogen Energy* **45**, 3847–3869 (2020).

2.   Acar, C. & Dincer, I. The potential role of hydrogen as a sustainable transportation fuel to combat global warming. *Int. J. Hydrogen Energy* **45**, 3396–3406 (2020).

3.   Ediger, V. An integrated review and analysis of multi-energy transition from fossil fuels to renewables. *Energy Procedia* **156**, 2–6 (2019).

4.   Acar, C. & Dincer, I. Review and evaluation of hydrogen production options for better environment. *J. Clean. Prod.* **218**, 835–849 (2019).

5.   Rosen, M. A. & Koohi-Fayegh, S. The prospects for hydrogen as an energy carrier: an overview of hydrogen energy and hydrogen energy systems. *Energy, Ecol. Environ.* **1**, 10–29 (2016).

6.   Staffell, I. *et al.* The role of hydrogen and fuel cells in the global energy system. *Energy Environ. Sci.* **12**, 463–491 (2019).

7.   Glenk, G. & Reichelstein, S. Economics of converting renewable power to hydrogen. *Nat. Energy* **4**, 216–222 (2019).

8.   Abdalla, A. M. *et al.* Hydrogen production, storage, transportation and key challenges with applications: A review. *Energy Convers. Manag.* **165**, 602–627 (2018).

9.   Mahidhara, G., Burrow, H., Sasikala, C. & Ramana, C. V. Biological hydrogen production: molecular and electrolytic perspectives. *World J. Microbiol. Biotechnol.* **35**, 1–13 (2019).

10.   Trchounian, K., Sawers, R. G. & Trchounian, A. Improving biohydrogen productivity by microbial dark- and photo-fermentations: Novel data and future approaches. *Renew. Sustain. Energy Rev.* **80**, 1201–1216 (2017).

11.   Hosseini, S. E. & Wahid, M. A. Hydrogen production from renewable and sustainable energy resources: Promising green energy carrier for clean development. *Renew. Sustain. Energy Rev.* **57**, 850–866 (2016).

12.   El-Shafie, M., Kambara, S. & Hayakawa, Y. Hydrogen Production Technologies Overview. *J. Power Energy Eng.* **07**, 107–154 (2019).

13.   Hosseini, S. E. & Wahid, M. A. Hydrogen from solar energy, a clean energy carrier from a sustainable source of energy. *Int. J. Energy Res.* **44**, 4110–4131 (2020).

References

14. Shahsavari, A. & Akbari, M. Potential of solar energy in developing countries for reducing energy-related emissions. *Renew. Sustain. Energy Rev.* **90**, 275–291 (2018).

15. Kannan, N. & Vakeesan, D. Solar energy for future world: - A review. *Renew. Sustain. Energy Rev.* **62**, 1092–1105 (2016).

16. Allakhverdiev, S. I. *et al.* Hydrogen photoproduction by use of photosynthetic organisms and biomimetic systems. *Photochem. Photobiol. Sci.* **8**, 148–156 (2009).

17. Fang, X., Kalathil, S. & Reisner, E. Semi-biological approaches to solar-to-chemical conversion. *Chem. Soc. Rev.* **49**, 4926–4952 (2020).

18. Volgusheva, A., Styring, S. & Mamedov, F. Increased photosystem II stability promotes H2 production in sulfur-deprived Chlamydomonas reinhardtii. *Proc. Natl. Acad. Sci. U. S. A.* **110**, 7223–7228 (2013).

19. Rowe, S. F. *et al.* Light-Driven H2 Evolution and C=C or C=O Bond Hydrogenation by Shewanella oneidensis: A Versatile Strategy for Photocatalysis by Nonphotosynthetic Microorganisms. *ACS Catal.* **7**, 7558–7566 (2017).

20. Heinekey, D. M. Hydrogenase enzymes: Recent structural studies and active site models. *J. Organomet. Chem.* **694**, 2671–2680 (2009).

21. Kornienko, N., Zhang, J. Z., Sakimoto, K. K., Yang, P. & Reisner, E. Interfacing nature's catalytic machinery with synthetic materials for semi-artificial photosynthesis. *Nat. Nanotechnol.* **13**, 890–899 (2018).

22. Brown, K. A. & King, P. W. Coupling biology to synthetic nanomaterials for semi-artificial photosynthesis. *Photosynth. Res.* **143**, 193–203 (2020).

23. Cestellos-Blanco, S., Zhang, H., Kim, J. M., Shen, Y. xiao & Yang, P. Photosynthetic semiconductor biohybrids for solar-driven biocatalysis. *Nat. Catal.* **3**, 245–255 (2020).

24. Lee, C. Y., Zou, J., Bullock, J. & Wallace, G. G. Emerging approach in semiconductor photocatalysis: Towards 3D architectures for efficient solar fuels generation in semi-artificial photosynthetic systems. *J. Photochem. Photobiol. C Photochem. Rev.* **39**, 142–160 (2019).

25. King, P. W. Designing interfaces of hydrogenase-nanomaterial hybrids for efficient solar conversion. *Biochim. Biophys. Acta - Bioenerg.* **1827**, 949–957 (2013).

26. Edwardes Moore, E., Andrei, V., Zacarias, S., Pereira, I. A. C. & Reisner, E. Integration of a Hydrogenase in a Lead Halide Perovskite Photoelectrode for Tandem Solar Water Splitting. *ACS Energy Lett.* **5**, 232–237 (2020).

27. Zhao, F. *et al.* A photosystem i monolayer with anisotropic electron flow enables Z-scheme like photosynthetic water splitting. *Energy Environ. Sci.* **12**, 3133–3143 (2019).

28. Tapia, C. *et al.* In Situ Determination of Photobioproduction of H2 by In2S3-[NiFeSe] Hydrogenase from Desulfovibrio vulgaris Hildenborough Using only

Visible Light. *ACS Catal.* **6**, 5691–5698 (2016).

29. Krasnovsky, A. A. & Nikandrov, V. V. The photobiocatalytic system: Inorganic semiconductors coupled to bacterial cells. *FEBS Lett.* **219**, 93–96 (1987).

30. Maruthamuthu, P., Muthu, S., Gurunathan, K., Ashokkumar, M. & Sastri, M. V. C. Photobiocatalysis: hydrogen evolution using a semiconductor coupled with photosynthetic bacteria. *Int. J. Hydrogen Energy* **17**, 863–866 (1992).

31. Gurunathan, K. Photobiocatalytic production of hydrogen using sensitized TiO2-MV2+ system coupled Rhodopseudomonas capsulata. *J. Mol. Catal. A Chem.* **156**, 59–67 (2000).

32. Honda, Y., Hagiwara, H., Ida, S. & Ishihara, T. Application to Photocatalytic H 2 Production of a Whole-Cell Reaction by Recombinant Escherichia coli Cells Expressing [FeFe] - Hydrogenase and Maturases Genes Angewandte. **55**, 8045–8048 (2016).

33. Honda, Y., Watanabe, M., Hagiwara, H., Ida, S. & Ishihara, T. Inorganic/whole-cell biohybrid photocatalyst for highly efficient hydrogen production from water. *Appl. Catal. B Environ.* **210**, 400–406 (2017).

34. Ramprakash, B. & Incharoensakdi, A. Light-driven biological hydrogen production by Escherichia coli mediated by TiO2 nanoparticles. *Int. J. Hydrogen Energy* **45**, 6254–6261 (2020).

35. Jiang, Y. & Tian, B. Inorganic semiconductor biointerfaces. *Nat. Rev. Mater.* **3**, 473–490 (2018).

36. da Costa, J. P. *et al.* Biological synthesis of nanosized sulfide semiconductors: current status and future prospects. *Appl. Microbiol. Biotechnol.* **100**, 8283–8302 (2016).

37. Raouf Hosseini, M. & Nasiri Sarvi, M. Recent achievements in the microbial synthesis of semiconductor metal sulfide nanoparticles. *Mater. Sci. Semicond. Process.* **40**, 293–301 (2015).

38. Ding, Y. *et al.* Nanorg Microbial Factories: Light-Driven Renewable Biochemical Synthesis Using Quantum Dot-Bacteria Nanobiohybrids. *J. Am. Chem. Soc.* **141**, 10272–10282 (2019).

39. Sakimoto, K. K., Wong, A. B. & Yang, P. Self-photosensitization of nonphotosynthetic bacteria for solar-to-chemical production. *Science (80-.).* **351**, 74–77 (2016).

40. Sakimoto, K. K. *et al.* Physical Biology of the Materials-Microorganism Interface. *J. Am. Chem. Soc.* **140**, 1978–1985 (2018).

41. Gonzales, J. N., Matson, M. M. & Atsumi, S. Nonphotosynthetic Biological CO2 Reduction. *Biochemistry* **58**, 1470–1477 (2019).

42. Jones, S. W. *et al.* CO 2 fixation by anaerobic non-photosynthetic mixotrophy for improved carbon conversion. *Nat. Commun.* **7**, (2016).

43.   Sahoo, P. C., Pant, D., Kumar, M., Puri, S. K. & Ramakumar, S. S. V. Material–Microbe Interfaces for Solar-Driven CO2 Bioelectrosynthesis. *Trends Biotechnol.* **1**, (2020).

44.   Lee, Y. V. & Tian, B. Learning from Solar Energy Conversion: Biointerfaces for Artificial Photosynthesis and Biological Modulation. *Nano Lett.* **19**, 2189–2197 (2019).

45.   Guo, Z., Richardson, J. J., Kong, B. & Liang, K. Nanobiohybrids: Materials approaches for bioaugmentation. *Sci. Adv.* **6**, 1–17 (2020).

46.   Cestellos-Blanco, S., Zhang, H. & Yang, P. Solar-driven carbon dioxide fixation using photosynthetic semiconductor bio-hybrids. *Faraday Discuss.* **215**, 54–65 (2019).

47.   Ye, J. *et al.* Light-driven carbon dioxide reduction to methane by Methanosarcina barkeri-CdS biohybrid. *Appl. Catal. B Environ.* **257**, 117916 (2019).

48.   Wang, B., Jiang, Z., Yu, J. C., Wang, J. & Wong, P. K. Enhanced CO2 reduction and valuable C2+ chemical production by a CdS-photosynthetic hybrid system. *Nanoscale* **11**, 9296–9301 (2019).

49.   Kumar, M. *et al.* Photosensitization of electro-active microbes for solar assisted carbon dioxide transformation. *Bioresour. Technol.* **272**, 300–307 (2019).

50.   Wang, B. *et al.* Enhanced Biological Hydrogen Production from Escherichia coli with Surface Precipitated Cadmium Sulfide Nanoparticles. *Adv. Energy Mater.* **7**, 1–10 (2017).

51.   Jiang, Z. *et al.* AgInS2/In2S3 heterostructure sensitization of Escherichia coli for sustainable hydrogen production. *Nano Energy* **46**, 234–240 (2018).

52.   Wei, W. *et al.* A surface-display biohybrid approach to light-driven hydrogen production in air. *Sci. Adv.* **4**, 1–7 (2018).

53.   Muyzer, G. & Stams, A. J. M. The ecology and biotechnology of sulphate-reducing bacteria. *Nat. Rev. Microbiol.* **6**, 441–454 (2008).

54.   Pereira, I. A. C. *et al.* A comparative genomic analysis of energy metabolism in sulfate reducing bacteria and archaea. *Front. Microbiol.* **2**, 1–22 (2011).

55.   Martins, M. & Pereira, I. A. C. Sulfate-reducing bacteria as new microorganisms for biological hydrogen production. *Int. J. Hydrogen Energy* **38**, 12294–12301 (2013).

56.   Martins, M. *et al.* Electron transfer pathways of formate-driven H2 production in Desulfovibrio. *Appl. Microbiol. Biotechnol.* **100**, 8135–8146 (2016).

57.   Korbekandi, H., Iravani, S. & Abbasi, S. Production of nanoparticles using organisms Production of nanoparticles using organisms. *Crit. Rev. Biotechnol.* **29**, 279–306 (2009).

58.   Heidelberg, J. F. *et al.* The genome sequence of the anaerobic, sulfate-reducing bacterium Desulfovibrio vulgaris Hildenborough. *Nat. Biotechnol.* **22**, 554–559 (2004).

59. Martins, M., Mourato, C. & Pereira, I. A. C. Desulfovibrio vulgaris Growth Coupled to Formate-Driven H2 Production. *Environ. Sci. Technol.* **49**, 14655–14662 (2015).

60. Valente, F. M. A. *et al.* Hydrogenases in Desulfovibrio vulgaris Hildenborough: Structural and physiologic characterisation of the membrane-bound [NiFeSe] hydrogenase. *J. Biol. Inorg. Chem.* **10**, 667–682 (2005).

61. Marques, M. C., Coelho, R., De Lacey, A. L., Pereira, I. A. C. & Matias, P. M. The three-dimensional structure of [nifese] hydrogenase from desulfovibrio vulgaris hildenborough: A hydrogenase without a bridging ligand in the active site in its oxidised, 'as-isolated' state. *J. Mol. Biol.* **396**, 893–907 (2010).

62. Martins, M. *et al.* Biogenic platinum and palladium nanoparticles as new catalysts for the removal of pharmaceutical compounds. *Water Res.* **108**, 160–168 (2017).

63. Deng, X., Dohmae, N., Kaksonen, A. H. & Okamoto, A. Biogenic Iron Sulfide Nanoparticles to Enable Extracellular Electron Uptake in Sulfate-Reducing Bacteria. *Angew. Chemie* **132**, 6051–6055 (2020).

64. Wu, X. *et al.* A role for microbial palladium nanoparticles in extracellular electron transfer. *Angew. Chemie - Int. Ed.* **50**, 427–430 (2011).

65. Eaktasang, N., Kang, C. S., Ryu, S. J., Suma, Y. & Kim, H. S. Enhanced current production by electroactive biofilm of sulfate-reducing bacteria in the microbial fuel cell. *Environ. Eng. Res.* **18**, 277–281 (2013).

66. Kang, C. S., Eaktasang, N., Kwon, D. Y. & Kim, H. S. Enhanced current production by Desulfovibrio desulfuricans biofilm in a mediator-less microbial fuel cell. *Bioresour. Technol.* **165**, 27–30 (2014).

67. Seol, E., Kim, S., Raj, S. M. & Park, S. Comparison of hydrogen-production capability of four different Enterobacteriaceae strains under growing and non-growing conditions. *Int. J. Hydrogen Energy* **33**, 5169–5175 (2008).

68. Vatsala, T. M. Hydrogen production from (cane-molasses) stillage by citrobacter freundii and its use in improving methanogenesis. *Int. J. Hydrogen Energy* **17**, 923–927 (1992).

69. Beckers, L., Hiligsmann, S., Hamilton, C., Masset, J. & Thonart, P. Fermentative hydrogen production by Clostridium butyricum CWBI1009 and Citrobacter freundii CWBI952 in pure and mixed cultures. *Biotechnol. Agron. Soc. Environ.* **14**, 541–548 (2010).

70. Hamilton, C. *et al.* Optimization of culture conditions for biological hydrogen production by Citrobacter freundii CWBI952 in batch, sequenced-batch and semicontinuous operating mode. *Int. J. Hydrogen Energy* **35**, 1089–1098 (2010).

71. Xu, S. & Liu, H. New exoelectrogen Citrobacter sp. SX-1 isolated from a microbial fuel cell. *J. Appl. Microbiol.* **111**, 1108–1115 (2011).

72. Feng, C. *et al.* Characterization of exoelectrogenic bacteria enterobacter strains isolated from a microbial fuel cell exposed to copper shock load. *PLoS One* **9**,

(2014).

73.   Huang, J. *et al.* Exoelectrogenic Bacterium Phylogenetically Related to Citrobacter freundii, Isolated from Anodic Biofilm of a Microbial Fuel Cell. *Appl. Biochem. Biotechnol.* **175**, 1879–1891 (2014).

74.   Tracy, B. P., Jones, S. W., Fast, A. G., Indurthi, D. C. & Papoutsakis, E. T. Clostridia: The importance of their exceptional substrate and metabolite diversity for biofuel and biorefinery applications. *Curr. Opin. Biotechnol.* **23**, 364–381 (2012).

75.   Latifi, A., Avilan, L. & Brugna, M. Clostridial whole cell and enzyme systems for hydrogen production: current state and perspectives. *Appl. Microbiol. Biotechnol.* **103**, 567–575 (2019).

76.   Lin, P. Y. *et al.* Biological hydrogen production of the genus Clostridium: Metabolic study and mathematical model simulation. *Int. J. Hydrogen Energy* **32**, 1728–1735 (2007).

77.   Calusinska, M., Happe, T., Joris, B. & Wilmotte, A. The surprising diversity of clostridial hydrogenases: A comparative genomic perspective. *Microbiology* **156**, 1575–1588 (2010).

78.   Engel, M. *et al.* Clostridium Acetobutylicum's Connecting World: Cell Appendage Formation in Bioelectrochemical Systems. *ChemElectroChem* **7**, 414–420 (2020).

79.   Cheng, L., Xiang, Q., Liao, Y. & Zhang, H. CdS-Based photocatalysts. *Energy Environ. Sci.* **11**, 1362–1391 (2018).

80.   Li, X. *et al.* Engineering heterogeneous semiconductors for solar water splitting. *J. Mater. Chem. A* **3**, 2485–2534 (2015).

81.   Xiao, N. *et al.* The roles and mechanism of cocatalysts in photocatalytic water splitting to produce hydrogen. *Chinese J. Catal.* **41**, 642–671 (2020).

82.   Ran, J., Zhang, J., Yu, J., Jaroniec, M. & Qiao, S. Z. Earth-abundant cocatalysts for semiconductor-based photocatalytic water splitting. *Chem. Soc. Rev.* **43**, 7787–7812 (2014).

83.   Peng, W., Li, Y., Zhang, F., Zhang, G. & Fan, X. Roles of Two-Dimensional Transition Metal Dichalcogenides as Cocatalysts in Photocatalytic Hydrogen Evolution and Environmental Remediation. *Ind. Eng. Chem. Res.* **56**, 4611–4626 (2017).

84.   Cao, S., Piao, L. & Chen, X. Emerging Photocatalysts for Hydrogen Evolution. *Trends Chem.* **2**, 57–70 (2020).

85.   Chang, K., Hai, X. & Ye, J. Transition Metal Disulfides as Noble-Metal-Alternative Co-Catalysts for Solar Hydrogen Production. *Adv. Energy Mater.* **6**, 1–21 (2016).

86.   Bullock, R. M. *et al.* Using nature's blueprint to expand catalysis with Earth-abundant metals. *Science (80-.).* **369**, (2020).

87.   Ma, B., Li, D., Wang, X. & Lin, K. Molybdenum-Based Co-catalysts in Photocatalytic Hydrogen Production: Categories, Structures, and Roles. *ChemSusChem* **11**, 3871–3881 (2018).

88. Zong, X. *et al.* Enhancement of photocatalytic H2 evolution on CdS by loading MoS2 as cocatalyst under visible light irradiation. *J. Am. Chem. Soc.* **130**, 7176–7177 (2008).

89. Chang, K. *et al.* MoS2/graphene cocatalyst for efficient photocatalytic H 2 evolution under visible light irradiation. *ACS Nano* **8**, 7078–7087 (2014).

90. Yin, X. L. *et al.* MoS2/CdS Nanosheets-on-Nanorod Heterostructure for Highly Efficient Photocatalytic H2 Generation under Visible Light Irradiation. *ACS Appl. Mater. Interfaces* **8**, 15258–15266 (2016).

91. Yang, Y. *et al.* Simultaneous Realization of Enhanced Photoactivity and Promoted Photostability by Multilayered MoS2 Coating on CdS Nanowire Structure via Compact Coating Methodology. *ACS Appl. Mater. Interfaces* **9**, 6950–6958 (2017).

92. Kadam, S. R. *et al.* Unique CdS@MoS2 Core Shell Heterostructure for Efficient Hydrogen Generation Under Natural Sunlight. *Sci. Rep.* **9**, 1–10 (2019).

93. Zong, X. *et al.* Photocatalytic H2 evolution on CdS loaded with WS2 as cocatalyst under visible light irradiation. *J. Phys. Chem. C* **115**, 12202–12208 (2011).

94. Zhong, Y., Zhao, G., Ma, F., Wu, Y. & Hao, X. Utilizing photocorrosion-recrystallization to prepare a highly stable and efficient CdS/WS2 nanocomposite photocatalyst for hydrogen evolution. *Appl. Catal. B Environ.* **199**, 466–472 (2016).

95. Zhang, K., Fujitsuka, M., Du, Y. & Majima, T. 2D/2D Heterostructured CdS/WS2 with Efficient Charge Separation Improving H2 Evolution under Visible Light Irradiation. *ACS Appl. Mater. Interfaces* **10**, 20458–20466 (2018).

96. Xu, D. *et al.* High Yield Exfoliation of WS2 Crystals into 1-2 Layer Semiconducting Nanosheets and Efficient Photocatalytic Hydrogen Evolution from WS2/CdS Nanorod Composites. *ACS Appl. Mater. Interfaces* **10**, 2810–2818 (2018).

97. Li, C., Wang, H., Naghadeh, S. B., Zhang, J. Z. & Fang, P. Visible light driven hydrogen evolution by photocatalytic reforming of lignin and lactic acid using one-dimensional NiS/CdS nanostructures. *Appl. Catal. B Environ.* **227**, 229–239 (2018).

98. Guan, S., Fu, X., Zhang, Y. & Peng, Z. NiS modified CdS nanowires for photocatalytic H2 evolution with exceptionally high efficiency. *Chem. Sci.* **9**, 1574–1585 (2018).

99. Zhou, X., Sun, H., Zhang, H. & Tu, W. One-pot hydrothermal synthesis of CdS/NiS photocatalysts for high H2 evolution from water under visible light. *Int. J. Hydrogen Energy* **42**, 11199–11205 (2017).

100. Zhang, W., Wang, Y., Wang, Z., Zhong, Z. & Xu, R. Highly efficient and noble metal-free NiS/CdS photocatalysts for H 2 evolution from lactic acid sacrificial solution under visible light. *Chem. Commun.* **46**, 7631–7633 (2010).

101. Huisman, J. L., Schouten, G. & Schultz, C. Biologically produced sulphide for purification of process streams, effluent treatment and recovery of metals in the metal and mining industry. *Hydrometallurgy* **83**, 106–113 (2006).

References

102. Leong, J. Y. *et al.* Advances in fabricating spherical alginate hydrogels with controlled particle designs by ionotropic gelation as encapsulation systems. *Particuology* **24**, 44–60 (2016).

103. Smrdel, P., Bogataj, M. & Mrhar, A. The influence of selected parameters on the size and shape of alginate beads prepared by ionotropic gelation. *Sci. Pharm.* **76**, 77–89 (2008).

104. Ahirrao, S., Gide, P., Shrivastav, B. & Sharma, P. Ionotropic Gelation: A Promising Cross Linking Technique for Hydrogels. *Res. Rev. J. Pharm. Nanotechnology}* **2**, 1–6 (2014).

105. Dong, G. *et al.* Cadmium sulfide nanoparticles-assisted intimate coupling of microbial and photoelectrochemical processes: Mechanisms and environmental applications. *Sci. Total Environ.* **740**, 140080 (2020).

106. Pellegrin, Y. & Odobel, F. Sacrificial electron donor reagents for solar fuel production. *Comptes Rendus Chim.* **20**, 283–295 (2017).

107. Hernández-Gordillo, A. *et al.* Dependence of the photoactivity of CdS prepared in butanol-ethylenediamine mixture in function of different sacrificial electron donors. *Catal. Today* **341**, 59–70 (2020).

108. Yu, H., Huang, X., Wang, P. & Yu, J. Enhanced Photoinduced-Stability and Photocatalytic Activity of CdS by Dual Amorphous Cocatalysts: Synergistic Effect of Ti(IV)-Hole Cocatalyst and Ni(II)-Electron Cocatalyst. *J. Phys. Chem. C* **120**, 3722–3730 (2016).

109. Durán-Pérez, J. F. *et al.* A Kinetic Model of Photocatalytic Hydrogen Production Employing a Hole Scavenger. *Chem. Eng. Technol.* **42**, 874–881 (2019).

110. Poole, L. B. The Basics of Thiols and Cysteines in Redox Biology and Chemistry. *Free Radic. Biol. Med.* **80**, 148–157 (2015).

111. Ralph, T. R., Hitchman, M. L., Millington, J. P. & Walsh, F. C. The electrochemistry of l-cystine and l-cysteine. Part 1: Thermodynamic and kinetic studies. *J. Electroanal. Chem.* **375**, 1–15 (1994).

112. Jocelyn, P. C. The Standard Redox Potential of Cysteine-Cystine from the Thiol-Disulphide Exchange Reaction with Glutathione and Lipoic Acid. *Eur. J. Biochem.* **2**, 327–331 (1967).

113. Opoku, F., Govender, K. K., van Sittert, C. G. C. E. & Govender, P. P. Recent Progress in the Development of Semiconductor-Based Photocatalyst Materials for Applications in Photocatalytic Water Splitting and Degradation of Pollutants. *Adv. Sustain. Syst.* **1**, 1–24 (2017).

114. Rabaey, K. & Rozendal, R. A. Microbial electrosynthesis - Revisiting the electrical route for microbial production. *Nat. Rev. Microbiol.* **8**, 706–716 (2010).

115. Chen, B.-Y. Deciphering Electron Shuttles for Bioremediation and Beyond. *Am. J. Chem. Eng.* **4**, 114–121 (2016).

116. Ding, J. *et al.* Viologen-inspired functional materials: Synthetic strategies and applications. *J. Mater. Chem. A* **7**, 23337–23360 (2019).

117. L. K. Cadman, M. F. M. and A. & D. Burrows. Inclusion of viologen cations leads to switchable metal-organic frameworks. *Faraday Discuss* (2020) doi:10.19009/jjacg.34.4_240.

118. Striepe, L. & Baumgartner, T. Viologens and Their Application as Functional Materials. *Chem. - A Eur. J.* **23**, 16924–16940 (2017).

119. Stroyuk, O. L., Rayevska, O. Y., Kozytskiy, A. V. & Kuchmiy, S. Y. Electron energy factors in photocatalytic methylviologen reduction in the presence of semiconductor nanocrystals. *J. Photochem. Photobiol. A Chem.* **210**, 209–214 (2010).

120. Sanchez, M. L. K., Wu, C. H., Adams, M. W. W. & Brian Dyer, R. Optimizing electron transfer from CdSe QDs to hydrogenase for photocatalytic H2 production. *Chem. Commun.* **55**, 5579–5582 (2019).

121. Fang, Y. *et al.* Intermittent photocatalytic activity of single CdS nanoparticles. *Proc. Natl. Acad. Sci. U. S. A.* **114**, 10566–10571 (2017).

122. Yu, J., Yu, Y., Zhou, P., Xiao, W. & Cheng, B. Morphology-dependent photocatalytic H2-production activity of CdS. *Appl. Catal. B Environ.* **156–157**, 184–191 (2014).

123. Oh, E. *et al.* Meta-analysis of cellular toxicity for cadmium-containing quantum dots. *Nat. Nanotechnol.* **11**, 479–486 (2016).

124. Wang, A. & Crowley, D. E. Global gene expression responses to cadmium toxicity in Escherichia coli. *J. Bacteriol.* **187**, 3259–3266 (2005).

125. Hossain, S. T. & Mukherjee, S. K. Toxicity of cadmium sulfide (CdS) nanoparticles against Escherichia coli and HeLa cells. *J. Hazard. Mater.* **260**, 1073–1082 (2013).

126. Zhang, H. *et al.* Bacteria photosensitized by intracellular gold nanoclusters for solar fuel production. *Nat. Nanotechnol.* **13**, 900–905 (2018).

127. Wang, L., Schultz, M. & Matijević, E. Preparation and properties of uniform amorphous and crystalline colloidal nickel sulfide. *Colloid Polym. Sci.* **275**, 593–598 (1997).

128. Zhang, Z. J., Zhang, J. & Xue, Q. J. Synthesis and characterization of a molybdenum disulfide nanocluster. *J. Phys. Chem.* **98**, 12973–12977 (1994).

129. Larkum, A. W. D. Limitations and prospects of natural photosynthesis for bioenergy production. *Curr. Opin. Biotechnol.* **21**, 271–276 (2010).

130. Singh, L. & Wahid, Z. A. Methods for enhancing bio-hydrogen production from biological process: A review. *J. Ind. Eng. Chem.* **21**, 70–80 (2015).

131. Kumar, G. *et al.* Recent insights into the cell immobilization technology applied for dark fermentative hydrogen production. *Bioresour. Technol.* **219**, 725–737 (2016).

132. Sekoai, P. T. *et al.* Microbial cell immobilization in biohydrogen production: a short

overview. *Crit. Rev. Biotechnol.* **38**, 157–171 (2018).

133. Polakovič, M. *et al.* Progress in biocatalysis with immobilized viable whole cells: systems development, reaction engineering and applications. *Biotechnol. Lett.* **39**, 667–683 (2017).

134. Alkayyali, T., Cameron, T., Haltli, B., Kerr, R. G. & Ahmadi, A. Microfluidic and cross-linking methods for encapsulation of living cells and bacteria - A review. *Anal. Chim. Acta* **1053**, 1–21 (2019).

135. Duarte, J. C., Rodrigues, J. A. R., Moran, P. J. S., Valença, G. P. & Nunhez, J. R. Effect of immobilized cells in calcium alginate beads in alcoholic fermentation. *AMB Express* **3**, 1–8 (2013).

Appendices
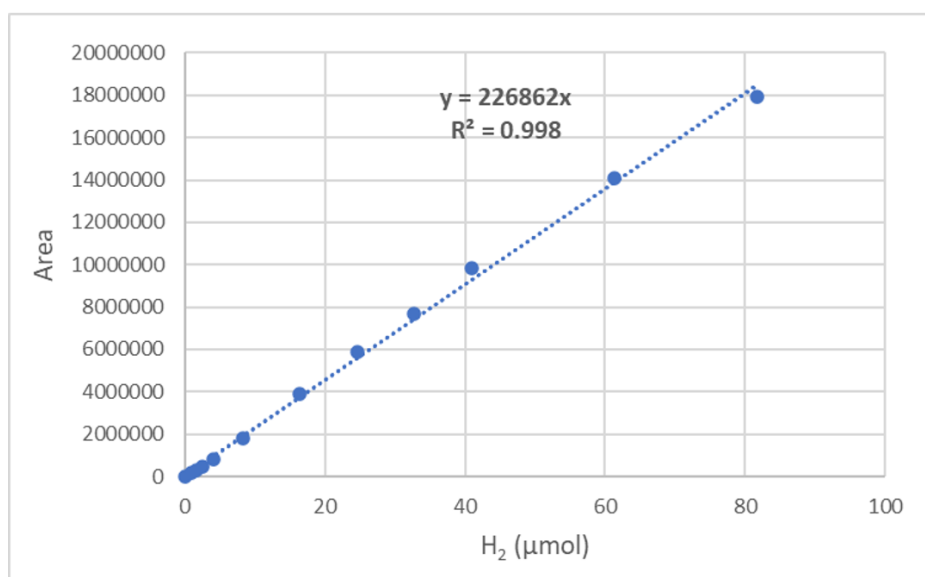
1) H_2 calibration curve

Table A1. - Values used to trace the H_2 calibration curve.

Volume H_2 (µL)	Area GC	H_2 (µmol)
0	0	0.000
20	176402	0.818
40	319382	1.636
60	467497	2.454
100	789991	4.089
200	1823368	8.179
400	3873735	16.358
600	5879349	24.537
800	7687413	32.716
1000	9812307	40.895
1500	14081280	61.342
2000	17944989	81.790

The H_2 calibration curve (**Figure A1.**) was traced based on the values presented in **Table A1**. The equation of the H_2 calibration curve is:

$$GC\ Area = 226862\ \times H_2\ (\mu mol) \quad \Leftrightarrow$$

$$\Leftrightarrow \boldsymbol{H_2\ (\mu mol) = 4 \times 10^{-6}\ GC\ Area,} \qquad \boldsymbol{R^2 = 0.998}$$

Figure A1. - H_2 calibration curved used to determine H_2 production.
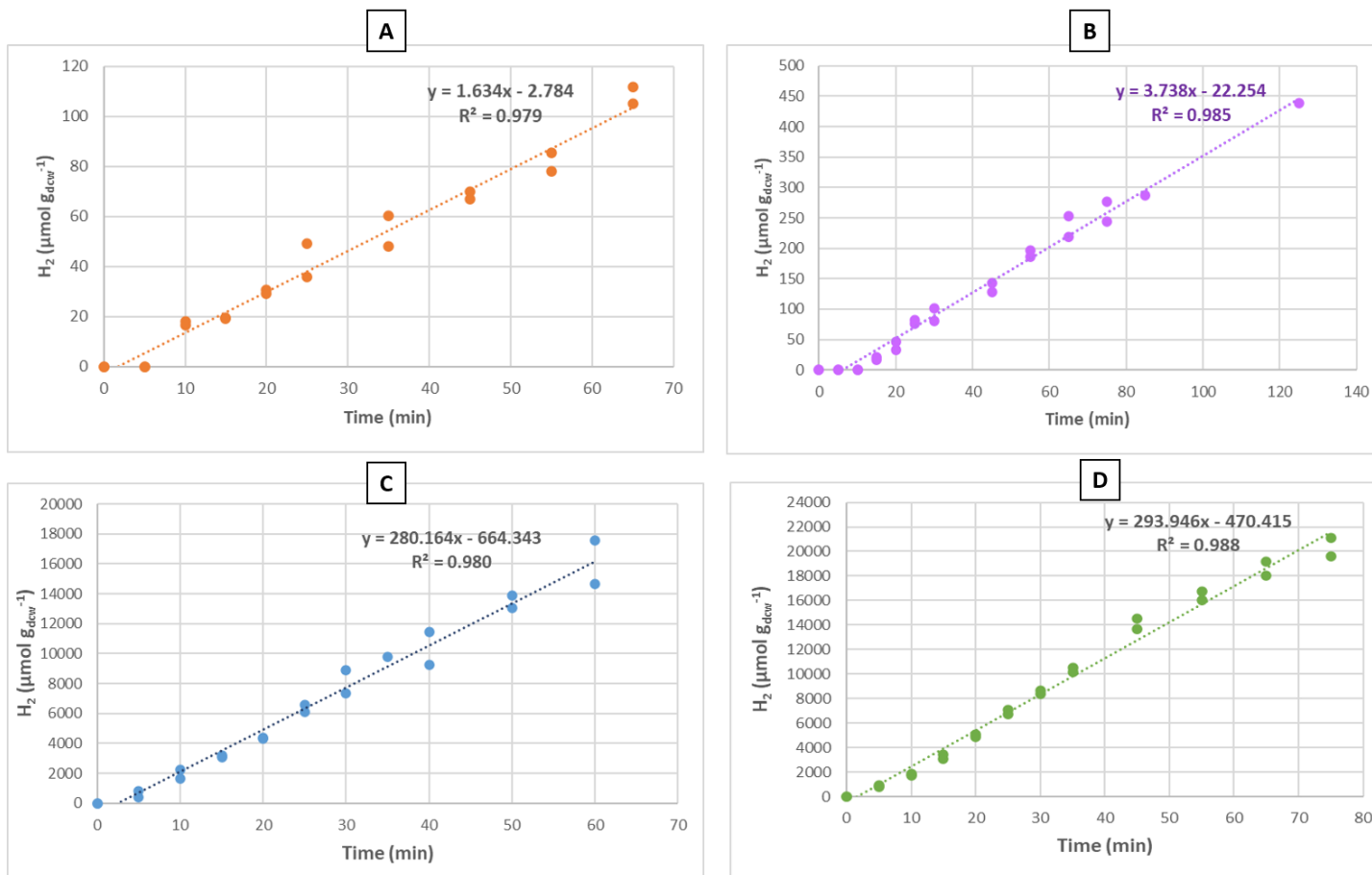
2) Determination of hydrogenases activity of whole-cells

Figure A2. - Hydrogenases activity of whole-cells: *Citrobacter freundii* (**A**), *Escherichia coli* (**B**), *Desulfovibrio desulfuricans* (**C**) and *Desulfovibrio vulgaris* (**D**).